Check for updates

ADVANCED FUNCTIONAL MATERIALS
www.afm-journal.de

Heterogeneity Governs 3D-Cultures of Clinically Relevant Microbial Communities

Daniela Peneda Pacheco, Federico Bertoglio, Cosmin Butnarasu, Natalia Suarez Vargas, Giuseppe Guagliano, Anna Ziccarelli, Francesco Briatico-Vangosa, Vincenzo Ruzzi, Stefano Buzzaccaro, Roberto Piazza, Sebastião van Uden, Elena Crotti, Sonja Visentin, Livia Visai,* and Paola Petrini**

The intrinsic heterogeneity of bacterial niches should be retained in in vitro cultures to represent the complex microbial ecology. As a case study, mucin-containing hydrogels -CF-Mu^{3}Gel - are generated by diffusion-induced gelation, bioinspired on cystic fibrosis (CF) mucus, and a microbial niche challenging current therapeutic strategies. At breathing frequency, CF-Mu^{3}Gel exhibits a G' and G'' equal to 24 and 3.2 Pa, respectively. Notably, CF-Mu^{3}Gel exhibits structural gradients with a gradual reduction of oxygen tension across its thickness (280–194 µmol L^{-1}). Over the culture period, a steep decline in oxygen concentration occurs just a few millimeters below the air–mucus interface in CF-Mu^{3}Gel, similar to those of CF airway mucus. Importantly, the distinctive features of CF-Mu^{3}Gel significantly influence bacterial organization and antimicrobial tolerance in mono- and co-cultures of *Staphylococcus aureus* and *Pseudomonas aeruginosa* that standard cultures are unable to emulate. The antimicrobial susceptibility determined in CF-Mu^{3}Gel corroborates the mismatch on the efficacy of antimicrobial treatment between planktonically cultured bacteria and those in patients. With this example-based research, new light is shed on the understanding of how the substrate influences microbial behavior, paving the way for improved fundamental microbiology studies and more effective drug testing and development.

1. Introduction

Structural, rheological, and compositional heterogeneity is a pervasive feature of most bacteria-hosting habitats. It has a significant impact on microbial organization, metabolic activity, and adopted pathways, and is further linked with energy consumption, gene expression and biomass production.[1] Within these complex 3D environments, individual bacteria are subjected to time-varying spatial gradients of nutrients, metabolites and oxygen (O_2) tension, all of which act as the driving forces of chemotaxis and aerotaxis. In multicellular communities, collective microbial dynamics contribute further to the heterogeneity of the environmental niche, generating a complex ecosystem characterized by both microbe–microbe and microbe–environment interaction dynamics. These features must somehow be rendered in in vitro models, and they are not reproducible with cultures in intrinsically homogeneous liquid media (planktonic conditions).

D. Peneda Pacheco, N. Suarez Vargas, G. Guagliano, A. Ziccarelli, F. Briatico-Vangosa, V. Ruzzi, S. Buzzaccaro, R. Piazza, S. van Uden, P. Petrini
Department of Chemistry
Materials and Chemical Engineering "Giulio Natta"
Politecnico di Milano
Piazza Leonardo da Vinci, 32, 20133 Milan, Italy
E-mail: paola.petrini@polimi.it

F. Bertoglio, L. Visai
Molecular Medicine Department (DMM)
Center for Health Technologies (CHT)
UdR INSTM
University of Pavia
Viale Taramelli 3/B, 27100 Pavia, Italy
E-mail: livia.visai@unipv.it

F. Bertoglio
School of Advanced Studies IUSS Pavia
Piazza della Vittoria, 15, 27100 Pavia, Italy

C. Butnarasu, S. Visentin
Molecular Biotechnology and Health Sciences Department
University of Turin
Via Nizza 52, 10126 Turin, Italy
E-mail: sonja.visentin@unito.it

The ORCID identification number(s) for the author(s) of this article can be found under https://doi.org/10.1002/adfm.202306116

© 2023 The Authors. Advanced Functional Materials published by Wiley-VCH GmbH. This is an open access article under the terms of the Creative Commons Attribution License, which permits use, distribution and reproduction in any medium, provided the original work is properly cited.

DOI: 10.1002/adfm.202306116

16163028, 2023, 50, Downloaded from https://advanced.onlinelibrary.wiley.com/doi/10.1002/adfm.202306116 by CochraneItalia, Wiley Online Library on [26/10/2025]. See the Terms and Conditions (https://onlinelibrary.wiley.com/terms-and-conditions) on Wiley Online Library for rules of use; OA articles are governed by the applicable Creative Commons License

Cystic fibrosis (CF) mucus is a challenging example of a heterogeneous microbial ecosystem. The presence of *Staphylococcus aureus* and *Pseudomonas aeruginosa* in CF mucus is generally associated with diminished lung function and more rapid pulmonary decline, but there is no consensus as to whether these bacteria are antagonistic or if *S. aureus* and *P. aeruginosa* can coexist in a complex microenvironment. Some studies indicate that early colonization by *P. aeruginosa* shows strong antagonism toward *S. aureus*,[2,3] through the secretion of a variety of anti-staphylococcal molecules and proteases that inhibit *S. aureus* growth and proliferation.[4,5] This process induces a metabolic transition of *S. aureus* from aerobic respiration to fermentation and eventually leads to a loss of *S. aureus* viability.[6] In response to this hostile environment, *S. aureus* may adapt to *P. aeruginosa* exoproducts by increasing biofilm formation and the presence of small colony variants.[5,7] Yet, other studies show that *S. aureus* supports colonization and pathogenicity of *P. aeruginosa*,[8] and that anaerobiosis is required for their coexistence.[9]

The need for novel models is imperative to address the contribution of the environment in bacterial cultures and co-cultures, particularly to enhance knowledge concerning mechanisms of bacterial colonization and how bacteria–bacteria and bacteria–environment interaction dynamics unfold in complex microbial ecosystems. Such models can help screen existing antimicrobial agents and support the development of new, patient-specific molecules, which are possibly closer to the actual clinical infections context, tackling infections occurring in mucus.[10] In vitro models exhibiting the key characteristics of the mucus environment, which, simultaneously, enable high throughput pharmacokinetics studies, would allow for a more effective screening of the most promising compounds early on in the drug discovery phase. These will additionally reduce the number of animals used during pre-clinical analyses.[11]

Existing in vitro models range from traditional methods, such as microtiter plates and dynamic systems,[12] to 3D printing of bacteria.[13,14] Co-cultures of *S. aureus* and *P. aeruginosa* have been performed using modified media in static[15] or dynamic conditions,[9,16–19] anoxia, microtiter plates,[20,21] Calgary biofilm device,[22] or even directly over mammalian cells.[6,23] The co-culture of these bacteria is of great importance, not only because of their mutual impact on behavior and metabolic activity, but also because some studies have shown that their interplay contributes to antimicrobial tolerance.[18,19,24,25] The challenge, however, is that existing models, despite shining some light on the behavior of these bacteria in 3D conditions, lack the heterogeneous environment that bacteria experience in the CF airway niche. Furthermore, it is important to acknowledge the significant role of mucus, as it contains a wide range of molecules with antimicrobial activity such as peptides, enzymes, antibodies, and various types of mucins.[26] The latter have a direct impact on bacterial behavior and their susceptibility to antimicrobial agents through the regulation of associated genes. Notably, mucins play a crucial role in the neutralization or elimination of invasive pathogenic bacteria, while also exhibiting immunomodulatory properties.[27,28] To provide a high throughput in vitro model that ensures interlaboratory reproducibility, it is important to rely on commercial reagents that are readily available in considerable amounts to offer consistent results. Now, there are mostly two sources of commercial mucins available in quantities that are compatible with these requirements, porcine stomach type III and mucin from bovine submaxillary glands. Mucin-containing structures composed of porcine gastric mucins have been recently proposed to culture microorganisms, to either culture intestinal microbiota[29] or co-culture *P. aeruginosa* and *Staphylococcus flexneri*.[30]

In this paper, we exploit a new approach based on a controlled diffusion of a crosslinking agent to generate a 3D structure that has the advantage of retaining spatial gradients, permitting microscopic-restructuring dynamics of the microstructure, and allowing for spatial control of O_2 content. This enabled the development of an in vitro model bioinspired on the microbiological environment of the CF airway mucus, supporting the study of the bacterial interplay within a heterogeneous microbial ecosystem. Gastric mucin was selected as mucin source, as this is composed of MUC5AC and MUC5B,[31] which have been reported to be also the main components of CF airway mucus.[32]

2. Results

2.1. Extracting the Key Features of Mucus to Reproduce a Heterogeneous Bacterial Environment

CF mucus models, CF-Mu^{3}Gel, were synthesized by slow calcium (Ca^{2+}) permeation through a membrane to slowly produce a 3D heterogeneous structure. CF-Mu^{3}Gel is predominantly composed of mucin and sodium chloride, whose ranges are within those reported in the literature for CF sputum.[32,33] CF-Mu^{3}Gel was produced using two common bacterial culture media, Müller Hinton broth (MHB) or Luria Bertani broth (LB). This reproduces the complex 3D mucus environment while retaining the fundamental composition of the culture media. The viscoelastic properties of the resultant CF-Mu^{3}Gel hydrogels were investigated through rheological characterization at the characteristic frequencies of both breathing (0.5 Hz) and ciliary beating (≈10 Hz)[34-36] and further compared to those reported for CF mucus.[37] Both storage (G') and dissipative (G'') components of the human mucus complex modulus impact its clearance. The capacity of the mucus to elastically store energy from the ciliary beating, quantified by G', allows the mucus to slide using this energy upon recoil of the cilia. Further, independently of the medium in which CF-Mu^{3}Gel was produced, the obtained G' was always higher than G'' confirming their gel-like structure, which prevents the mucus from flowing down the airway due to gravity forces. Herein, the viscoelastic properties of the hydrogels were not strongly affected by the different culture media, although CF-Mu^{3}Gel produced in MHB displayed closer characteristics to those of CF mucus reported in the literature

E. Crotti
Department of Food
Environmental and Nutritional Sciences (DeFENS)
University of Milan
Via Celoria 2, Milan 20133, Italy
L. Visai
Medicina Clinica-Specialistica
UOR5 Laboratorio di Nanotecnologie
ICS Maugeri
IRCCS
Via S. Boezio 28, Pavia 27100, Italy

© 2023 The Authors. Advanced Functional Materials published by Wiley-VCH GmbH

16163028, 2023, 50, Downloaded from https://advanced.onlinelibrary.wiley.com/doi/10.1002/adfm.202306116 by Cochraneltalia, Wiley Online Library on [26/10/2025]. See the Terms and Conditions (https://onlinelibrary.wiley.com/terms-and-conditions) on Wiley Online Library for rules of use; OA articles are governed by the applicable Creative Commons License

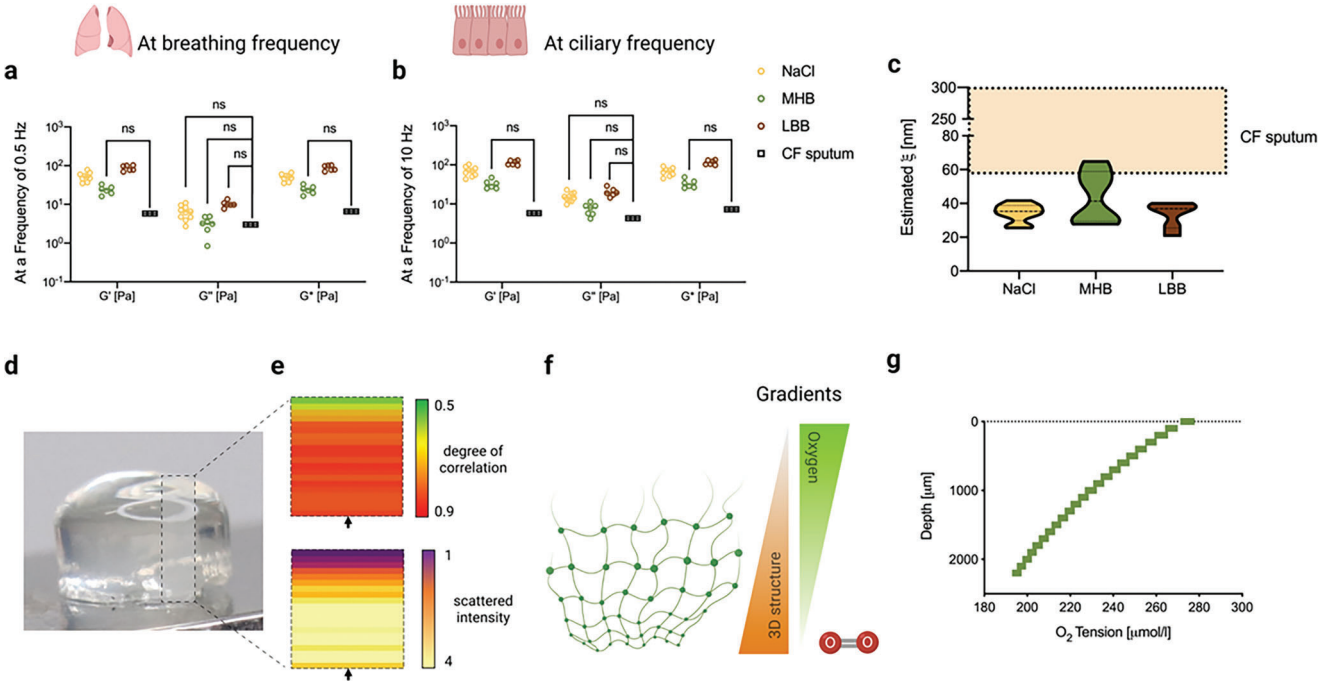

Figure 1. Topographical, chemical, and physical features of CF-Mu^{3}Gel. ab) Viscoelastic properties of CF-Mu^{3}Gel in function of production media: storage modulus, G' (Pa), dissipative modulus, G'' (Pa), and complex dynamic modulus, G^* (Pa) of CF-Mu^{3}Gel was analyzed at a, breathing (≈0.5 Hz); and ciliary beating frequency (10 Hz; $n \geq 6$) (b). The rheological data were analyzed using the two-way ANOVA. Significant differences were set for $^*p < 0.05$. A minimum of six independent samples were analyzed per formulation ($n \geq 6$). *ns* means no statistical differences were found between the viscoelastic properties of the different formulations of CF-Mu^{3}Gel and those of CF sputum reported by Yuan et al. (2015).[37] c) Dependency of mesh size (ξ) of CF-Mu^{3}Gel on media in which this was produced estimated by combining the Generalized Maxwell Model with the rubber elasticity theory ($n \geq 6$). d) Macroscopic image of CF-Mu^{3}Gel produced with 0.16% (w/v) Ca^{2+} ions. e) Correlation (top) and intensity (bottom) maps c_i of a region of ≈2.83 × 2.66 mm, obtained after 20 h of crosslinking reaction for a CF-Mu^{3}Gel. The correlation index is evaluated for a delay of 60 s and the intensity is normalized to its value at the top. f) Schematic representation of both topographical and O_2 gradients exhibited through the 3D structure of CF-Mu^{3}Gel. g) Heterogeneous distribution of O_2 tension through the structure of sterile CF-Mu^{3}Gel ($n = 5$).

(**Figure 1**a,b).[37] As CF mucus characteristics vary, not only between patients, but also within a single patient in a short period of time,[38-42] the concentration of Ca^{2+} ions was varied to produce CF-Mu^{3}Gel with viscoelastic properties (Figure S1a,b, Supporting Information) tailorable to the desired stiffness according to disease progression[43] or even patient-specific to support personalized pharmacological treatment. The average mesh size, estimated for all tested CF-Mu^{3}Gel formulations, decreased with increased concentration of Ca^{2+} ions (Figure S1c, Supporting Information). However, the CF-Mu^{3}Gel produced in MHB exhibited a closer mesh size to that reported for CF sputum than those produced in LB and NaCl (Figure 1c).[38] As a result, all further analyses were therefore performed on CF-Mu^{3}Gel produced in MHB (Figure 1d), as this maximized the representation of CF mucus structural properties.

Gradients have a tremendous impact on microbial behavior and though they are present in most of the human mucus, the methods to characterize them are scarce. Photon Correlation Imaging (PCI) combines dynamic light scattering with digital imaging and allows to study slow and spatially limited spontaneous restructuring dynamics of soft disordered solids. It was previously used to study the kinetic of the formation of hydrogels.[44] In this case, this unconventional technique was adapted to study structural gradients evaluating the different microscopic dynamics of the motion of the molecular chains resulting from the different crosslinking density (Figure S2, Supporting Information). PCI enabled the visualization of both gradients in the structure and microscopic dynamics of the CF-Mu^{3}Gel to be detected via scattered intensity and correlation maps, respectively. The correlation maps evidence that diffusion-controlled gelation produced hydrogels which were stiffer and almost dynamically arrested in the regions first exposed to Ca^{2+} ions (orange region, top map in Figure 1e, Figure S2, Supporting Information). The zones far from the diffusion inlet are more tenuous and display high degrees of spontaneous restructuring dynamics (green regions). Besides, CF-Mu^{3}Gel retains a gradual reduction of O_2 tension from top to bottom, decreasing from 280 to 194 µmol L^{-1} concerning y = 0–2300 µm, respectively (Figure 1g). In this way, PCI and microsensing techniques enabled the characterization of both topographical and O_2 gradients, respectively, throughout the 3D structure of CF-Mu^{3}Gel (Figure 1f).

2.2. Structural and O_2 Gradients Affect the Topographical Organization of *S. aureus* and *P. aeruginosa*

CF-Mu^{3}Gel kept its integrity up to the end of the test (48 h) when cultured with *S. aureus* and *P. aeruginosa*. After 72 h of incubation in different media, sterile CF-Mu^{3}Gel retained its dimensions

© 2023 The Authors. Advanced Functional Materials published by Wiley-VCH GmbH

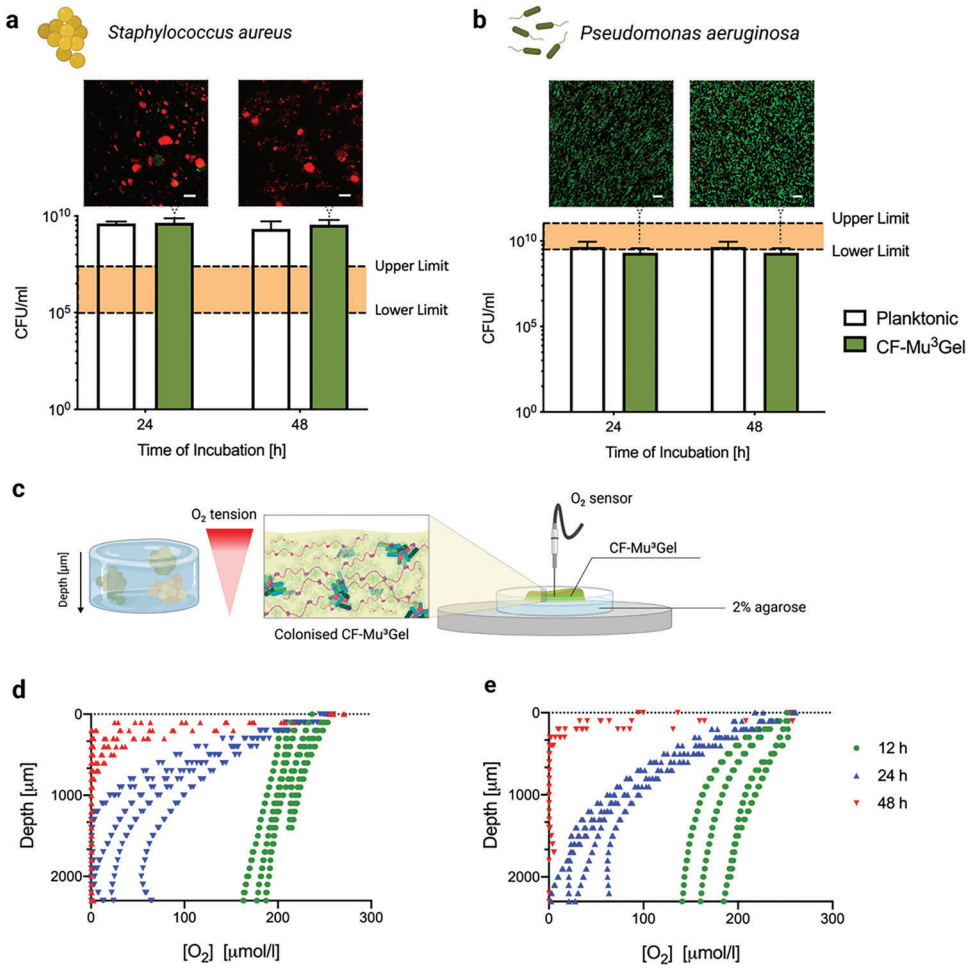

Figure 2. Mono-cultures of CF-Mu^{3}Gel with either *S. aureus* or *P. aeruginosa*. a,b) Bacteria viability, determined through Colony Forming Units (CFU), after incubating either *S. aureus* (a) or *P. aeruginosa* (b) with 10^3 bacteria for 24 and 48 h in CF-Mu^{3}Gel ($n = 9$) with the confocal microscopy images of colonized CF-Mu^{3}Gel for 24 and 48 h (the scale bar corresponds to 10 µm). The results obtained with CF-Mu^{3}Gel (green) were further compared with planktonic cultures (white). In (a) and (b), the shadowed region depicts the range of CFU mL^{-1} of each bacterium reported in the literature for pathological CF mucus.[45] A minimum of five independent samples were analyzed per bacterium ($n > 5$). No statistical differences were detected neither between both planktonic cultures and CF-Mu^{3}Gel nor between the same culturing system at different culturing periods. c) Experimental setup adopted to measure oxygen (O_2) tension through CF-Mu^{3}Gel colonized with either d) *S. aureus* or e) *P. aeruginosa* for 12 (green), 24 (blue), and 48 h (red) ($n = 5$).

with variations of 20% (weight) and 40% (thickness) on average when incubated in both isotonic and hypertonic media, and with variations of 44% (weight) and 200% (thickness) when incubated in hypotonic medium alone (Figure S1d,e, Supporting Information).

Mono-cultures of *S. aureus* and *P. aeruginosa* in CF-Mu^{3}Gel and planktonic conditions reached the stationary phase at 24 h with counts of ≈10^9 CFU mL^{-1} (**Figure 2**a,b). It is notable that an interlaboratory study showed a similar number for both bacteria after 24 h of culture, demonstrating that the results obtained in CF-Mu^{3}Gel are laboratory- and operator-independent (Figure S3, Supporting Information).

O_2 profiles across CF-Mu^{3}Gel indicated that, independently of the microorganism, O_2 content decreased in relation to the depth and extent to which the CF-Mu^{3}Gel was colonized, even after 12 h of culture (Figure 2d,e). This decrease was more pronounced for longer periods of incubation, and O_2 tension was progressively reduced to a completely anoxic zone, at ≈300 µm of depth, after 48 h of culture (Figure 2d,e).

Qualitative analyses of bacterial organization indicated that during the culture period, the number of *S. aureus* within CF-Mu^{3}Gel increased and exhibited depth-dependent differences in growth and in the presence of bacterial aggregates, these were visible after 24 h of culture (Figure 2a; Figure S4, Supporting Information) and increased in size with the progression of the time of culture (Figure S4, Supporting Information). Regardless of the observed position, a longer culture time resulted in a higher number of *P. aeruginosa* within the CF-Mu^{3}Gel (Figure 2b, Figure S5, Supporting Information). *S. aureus* and *P. aeruginosa* were able to migrate and colonize the whole thickness of CF-Mu^{3}Gel, with a higher number of bacteria at the top and bottom of CF-Mu^{3}Gel.

© 2023 The Authors. Advanced Functional Materials published by Wiley-VCH GmbH

16163028, 2023, 50, Downloaded from https://advanced.onlinelibrary.wiley.com/doi/10.1002/adfm.202306116 by Cochraneltalia, Wiley Online Library on [26/10/2025]. See the Terms and Conditions (https://onlinelibrary.wiley.com/terms-and-conditions) on Wiley Online Library for rules of use; OA articles are governed by the applicable Creative Commons License

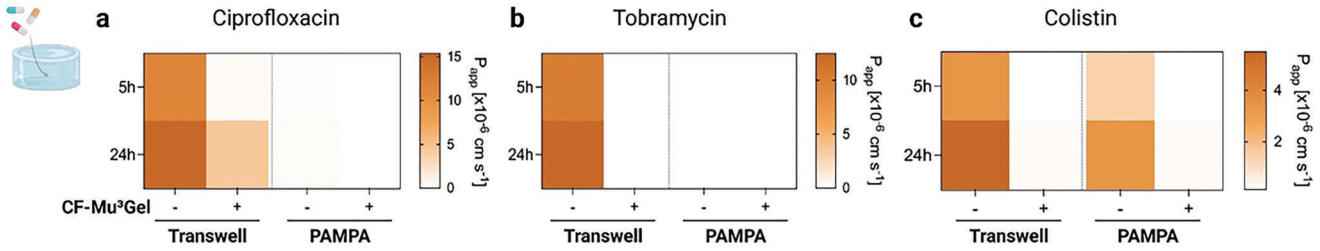

Figure 3. Permeability assessment of: a) ciprofloxacin; b) tobramycin; and c) colistin after 5 and 24 h through both Transwell supports or PAMPA membranes with (+) and without (–) CF-Mu^{3}Gel ($n = 3$).

2.3. CF-Mu^{3}Gel Governs the Permeability of Antimicrobial Agents

CF-Mu^{3}Gel was coupled with either Transwell supports or PAMPA (parallel artificial membrane permeability assays) membranes, widely used during permeability assessment[46] to evaluate the role of CF-Mu^{3}Gel on antimicrobial retention and consequent antimicrobial susceptibility. CF-Mu^{3}Gel strongly hindered the passage of the three antimicrobial agents (**Figure 3**), independently of the supporting system. The differences between Transwell supports and PAMPA were observable but were irrelevant when the effect of CF-Mu^{3}Gel is considered (Figure 3, Figure S7, Supporting Information).

2.4. Bacteria in CF-Mu^{3}Gel Resist Antimicrobial Treatment

The Minimal Inhibitory Concentration (MIC) of different antimicrobial agents (ciprofloxacin, tobramycin and colistin), which are commonly administered to CF patients with *S. aureus* and/or *P. aeruginosa* infections was assessed according to The European Committee on Antimicrobial Susceptibility Testing (EUCAST) guidelines (Figure S8, Supporting Information). The determined MIC values were the starting point to further treat bacteria incubated in CF-Mu^{3}Gel for 24 h.

A significant antimicrobial effect was observed when *S. aureus* was cultured under planktonic conditions (four-log$_{10}$ and six-log$_{10}$ decline of colonies with 1 and 10 MIC, respectively; **Figure 4**a,b). The antimicrobial treatment was less effective toward *S. aureus* cultured in CF-Mu^{3}Gel at short treatment times (two-log$_{10}$ and four-log$_{10}$ decline for 1 and 10 MIC, respectively; Figure 4a). When bacteria were cultured for extended periods, to simulate established infection conditions, prior to antimicrobial treatment, the number of *S. aureus* colonies in CF-Mu^{3}Gel remained constant, even when a high concentration of ciprofloxacin was used (10 MIC; Figure 4b). In contrast, a more pronounced antimicrobial effect was observed in *S. aureus* cultured in planktonic conditions, with a decline in colonies of two-log$_{10}$ and three-log$_{10}$ from 1 and 10 MIC, respectively, when compared with bacteria grown without antimicrobial treatment (Figure 4a).

P. aeruginosa was more resistant to antimicrobial treatment when cultured within CF-Mu^{3}Gel than in liquid medium (Figure 4c–e). In fact, in planktonic cultures, the number of CFU decreased progressively with increasing concentrations of both ciprofloxacin and tobramycin, resulting in a steep reduction of six-log$_{10}$ and nine-log$_{10}$ after 24 h of treatment with 1 and 10 MIC, respectively, when compared with the untreated control group (Figure 4c,d). In contrast, the concentration of 10 MIC tobramycin was found to be three times less effective against *P. aeruginosa* in CF-Mu^{3}Gel than in planktonic conditions (Figure 4d). Additionally, colistin treatment was found to be ineffective against bacteria grown within CF-Mu^{3}Gel, even at high concentrations, as it was not able to eradicate *P. aeruginosa* (Figure 4d), while bacteria cultured under planktonic conditions were only susceptible to 10 MIC of colistin.

2.5. *S. aureus* and *P. aeruginosa* Co-Exist and Compete in CF-Mu^{3}Gel in Different Culture Setups

Microbial ecosystems composed of *S. aureus* and *P. aeruginosa* coexisted in vitro in CF-Mu^{3}Gel, influencing each other's growth (**Figure 5**a–c) and topographical organization (Figure 5d–f), independent of the culture method used. As the timing of colonization may affect the way they interact, three different types of co-culture were simulated: (1) a contemporary co-culture of both *S. aureus* and *P. aeruginosa* for 24 h (Figure 5a,d); (2) a 24 h culture with *S. aureus* first, followed by a *P. aeruginosa* culture for another 24 h of incubation (Figure 5b,e); and finally (3) a 24 h culture with *P. aeruginosa* first, followed by *S. aureus* culture for another 24 h of incubation (Figure 5c,f). Contemporary co-culture provides both pathogens with equal conditions for them to thrive (Figure 5a). After 24 h of co-culture, both bacteria were present in CF-Mu^{3}Gel (Figure 5a), and these were able to colonize the 3D structure (Figure 5d). This was not observed in planktonic cultures, as *S. aureus* was not able to grow.

To reproduce CF airways microbial colonization timeline[48] the experimental setting (2) was used (*S. aureus* first). After 48 h of culture, both *S. aureus* and *P. aeruginosa* co-existed either in CF-Mu^{3}Gel or planktonic conditions (Figure 5b). The relative abundance of *S. aureus* in respect to *P. aeruginosa* was prevalent in planktonic conditions (Figure 5b).

When *P. aeruginosa* was first cultured in CF-Mu^{3}Gel, experimental setting (3), both *S. aureus* and *P. aeruginosa* co-existed within CF-Mu^{3}Gel, though the relative abundance of *S. aureus* was minor (Figure 5c). Under planktonic conditions, *P. aeruginosa* outcompeted *S. aureus* (Figure 5c).

The topographical organization in co-cultures indicated that both *S. aureus* and *P. aeruginosa* formed bacterial aggregates (Figure 5d–f). This was also observed in mono-cultures of *S. aureus* and *P. aeruginosa* within CF-Mu^{3}Gel (Figures S4–S6, Supporting Information). However, the aggregates of *P. aeruginosa*

© 2023 The Authors. Advanced Functional Materials published by Wiley-VCH GmbH

16163028, 2023, 50, Downloaded from https://advanced.onlinelibrary.wiley.com/doi/10.1002/adfm.202306116 by CochraneItalia, Wiley Online Library on [26/10/2025]. See the Terms and Conditions (https://onlinelibrary.wiley.com/terms-and-conditions) on Wiley Online Library for rules of use; OA articles are governed by the applicable Creative Commons License

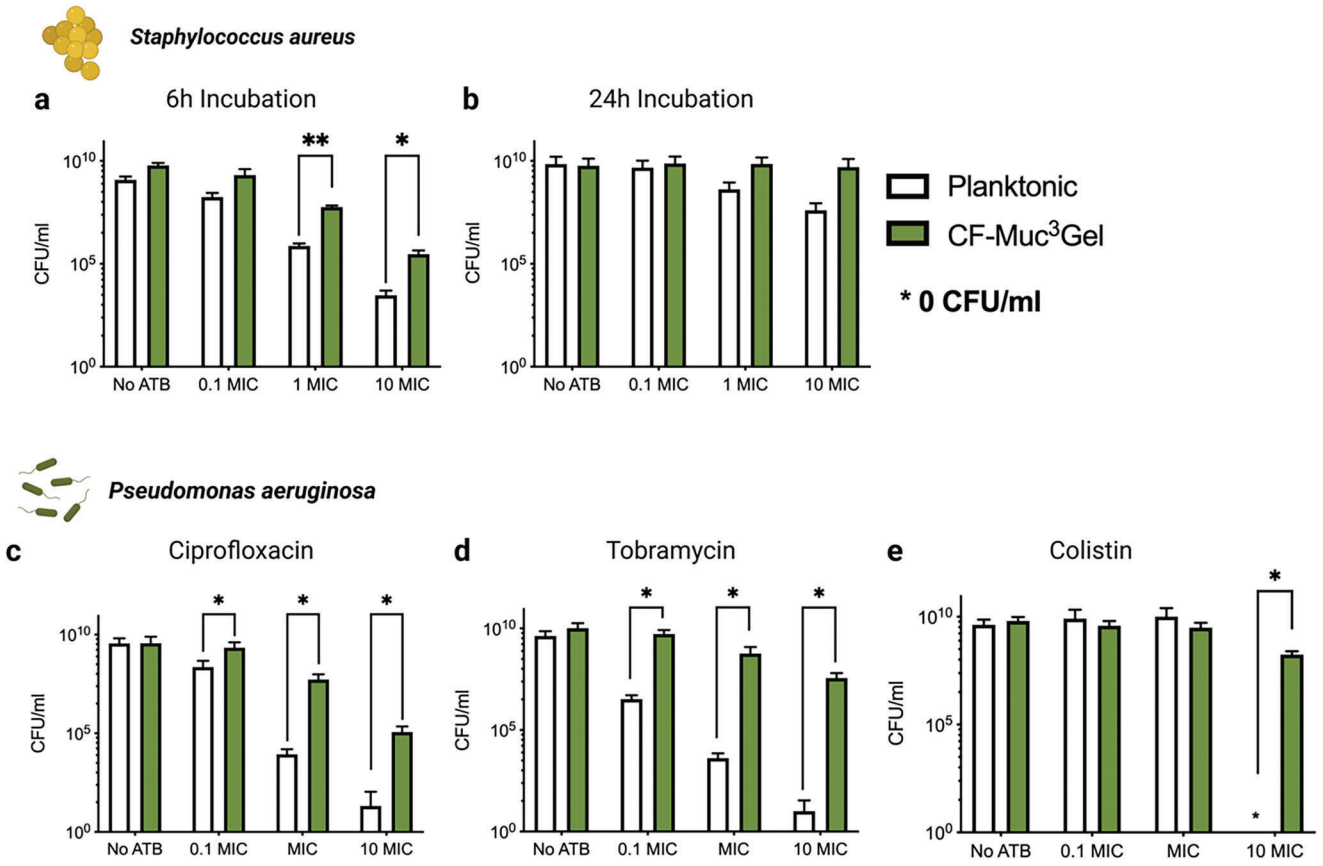

Figure 4. Antimicrobial treatment of CF-Mu^{3}Gel colonized with either *S. aureus* or *P. aeruginosa* for 24 h. Ciprofloxacin treatment of CF-Mu^{3}Gel colonized with *S. aureus* for a) 6; and b) 24 h. 0.1, 1, and 10 MIC correspond to 0.05, 0.5, and 5 mg L^{-1}, respectively. Antimicrobial treatment of CF-Mu^{3}Gel colonized with *P. aeruginosa* for 24 h followed by treatment with: c) ciprofloxacin; d) tobramycin; and e) colistin. In the case of ciprofloxacin, 0.1, 1, and 10 MIC correspond to 0.05, 0.5, and 5 mg L^{-1}, respectively, while for both tobramycin and colistin 0.1, 1, and 10 MIC correspond to 0.8, 8, and 80 mg L^{-1}, respectively. No ATB means that no antimicrobial treatment was performed. Planktonic cultures of *S. aureus* and *P. aeruginosa* were used as controls of the experiment. 0 CFU mL^{-1} indicates that no CFU were detected. All data were analyzed using the one-way ANOVA. Significant differences were set for $*p < 0.05$; and $**p < 0.01$. A minimum of five independent samples were analyzed per formulation ($n \geq 5$).

produced in experimental setting (3) (Figure 5f) were larger than those observed in experimental setting (2) (Figure 5e), possibly due to the longer culture time of *P. aeruginosa*.

When *S. aureus* was cultured first, mimicking the microbial colonization timeline of CF airways,[38] experimental setting (2), the co-existence of the two bacteria species impacted their susceptibility to ciprofloxacin treatment. In CF-Mu^{3}Gel, no differences were observed in the number of either bacteria species in the co-cultures that were treated with the tested ciprofloxacin concentrations (Figure 6b,d). Interestingly, the bacterial survival rates in CF-Mu^{3}Gel of both *S. aureus* and *P. aeruginosa* after ciprofloxacin treatment were higher when in co-cultures than they were in mono-cultures. The opposite was found to be the case in *S. aureus* co-cultured in planktonic conditions (**Figure 6**a).

3. Discussion

By replicating key features of the microbial ecology of a specific environment, a 3D-substrate able to support the growth of mono- and poly-microbial communities was developed. The challenging environment of CF mucus airway was taken as inspiration due to its complex ecology. The key features governing the microbial behavior were identified in the 3D-structural gradients, physical and chemical composition, O_2 distribution, and its ability to function as a barrier to antimicrobial diffusion, antagonistic phenomena and bacteria susceptibility to antimicrobials.

The intention was to model the airway CF mucus by replicating the viscoelastic properties and mucin content that were previously reported.[33,37,49] The viscoelastic properties of CF-Mu^{3}Gel increased with frequency (Figure 1a,b). This has been linked to limited mucus clearance creating an environment for infections to thrive.[3,24,50] The production of gradients within hydrogels is not a trivial issue, and so is their characterization.[51] Specifically challenging to study are the gradients at the molecular level, which are crucial for the organization of both microbial niches and biological tissues. Here, we employed PCI to gain information about the molecular structure of the produced hydrogels, and it was possible to evaluate the change in restructuring dynamics related to the gradient of crosslinking. The gradient structure of CF-Mu^{3}Gel (Figure 1e,f) is similar to the structure of CF airway mucus, where stagnating mucins form a higher number of entanglements at the lower strata of the mucus than at the

© 2023 The Authors. Advanced Functional Materials published by Wiley-VCH GmbH

16163028, 2023, 50, Downloaded from https://advanced.onlinelibrary.wiley.com/doi/10.1002/adfm.202306116 by CochraneItalia, Wiley Online Library on [26/10/2025]. See the Terms and Conditions (https://onlinelibrary.wiley.com/terms-and-conditions) on Wiley Online Library for rules of use; OA articles are governed by the applicable Creative Commons License

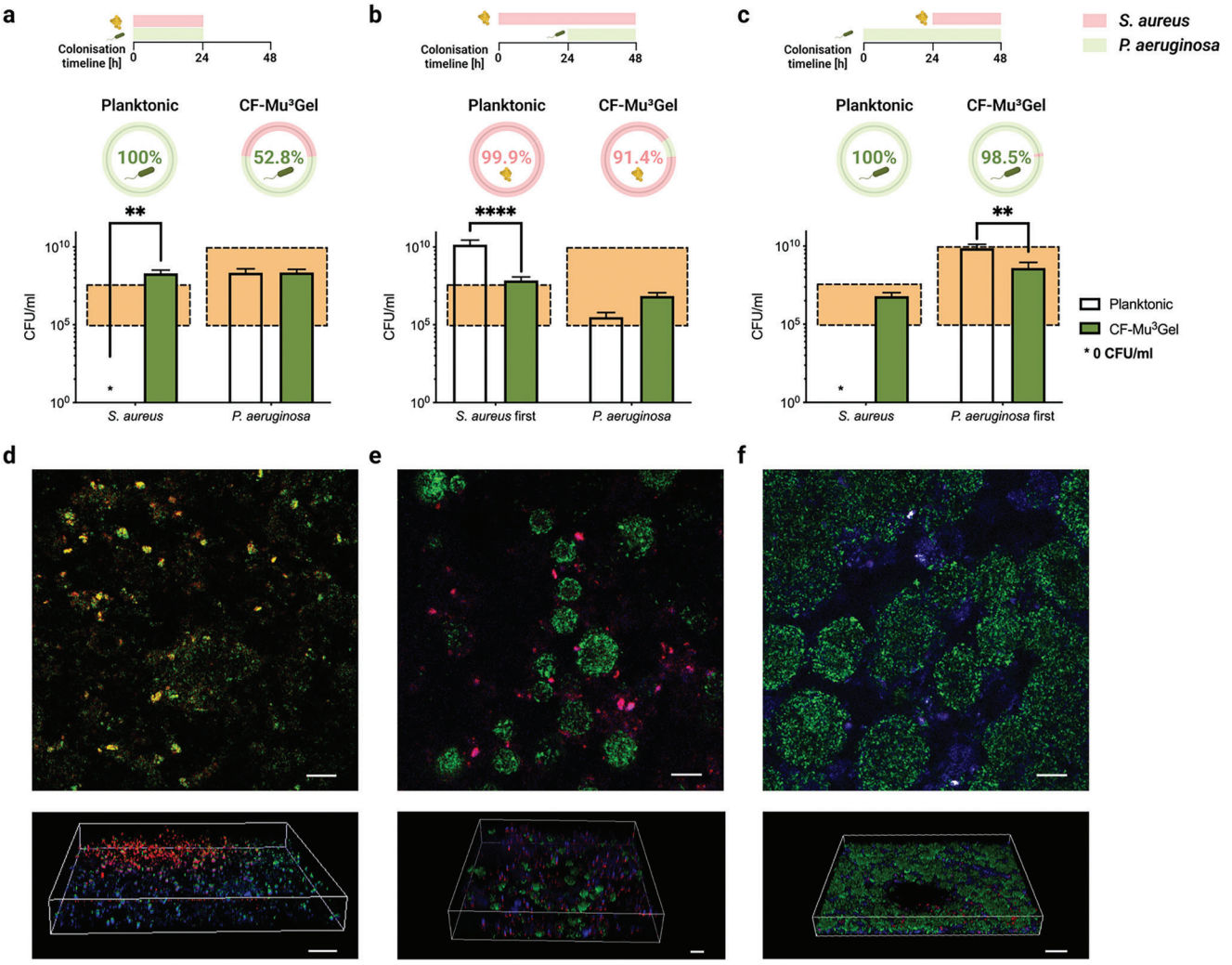

Figure 5. Co-cultures of CF-Mu^{3}Gel with both *S. aureus* and *P. aeruginosa* following three different co-culture settings: a,d-1) contemporary culture of both *S. aureus* (in light red) and *P. aeruginosa* (in light green) for 24 h; b,e-2) first culture with *S. aureus* for 24 h followed by *P. aeruginosa* culture for other 24 h; and finally, c,f-3) culture with *P. aeruginosa* first for 24 h, after which *S. aureus* is added and incubated for further 24 h. Bacteria numbers determined in CF-Mu^{3}Gel (green) were further compared with planktonic cultures (white) (a–c). The shadowed region depicts the range of CFU mL^{-1} of each bacterium reported in the literature for pathological CF mucus.[45,47] All data were analyzed using two-way ANOVA. Significant differences were set for $^*p < 0.05$; $^{**}p < 0.01$; $^{***}p < 0.001$; $^{****}p < 0.0001$. A minimum of five independent samples were analyzed per formulation ($n \geq 5$). The relative abundance of *S. aureus* in respect to *P. aeruginosa* per each experimental setting is depicted in the pie charts in the upper part of (a–c). Confocal microscopy analyses of CF-Mu^{3}Gel co-colonized with both DsRed-fluorescent *S. aureus* (fluorescent red) and GFP-fluorescent *P. aeruginosa* (fluorescent green) (d–f). Co-colonized CF-Mu^{3}Gel was further stained with Hoechst 33342 to depict total bacteria (in blue) and 3D reconstruction are also provided. The scale bar corresponds to 10 µm.

airway–mucus interface. The gelation, induced by diffusion of the crosslinking agent, results in reproducible gradients of structural stiffness, spontaneous restructuring power, and receptiveness to O_2.

O_2 gradients within native microbial ecosystems are known to affect bacterial metabolic activity and influence their susceptibility to antimicrobial agents. The O_2 gradient is a unique feature of CF-Mu^{3}Gel, with a lower O_2 tension at the bottom and a higher O_2 tension at the top that is linked to low crosslinking density (Figure 1f,g). This profile is related to the diffusion of O_2 in hydrogels, dependent on bound, free, and interfacial water content, mesh size, and crosslinking density.[52] Given that CF-Mu^{3}Gel exhibits a gradient structure with a tighter mesh at the bottom than at the top (Figure 1e), higher water-to-polymer ratios are found at the top than at the bottom (Figure 1g). Consequently, higher levels of O_2 are available at the top for bacteria metabolism.

CF-Mu^{3}Gel sustained the growth of *S. aureus* and *P. aeruginosa* (Figure 2a,b, Figure 4a–e "No ATB"). In CF-Mu^{3}Gel, the *P. aeruginosa* number was comparable to the numbers found in the lungs of CF patients (10^8–10^{10} bacteria mL^{-1}), while the number of *S. aureus* was higher.[45] *S. aureus* aggregates were found to increase in number and size over time in CF-Mu^{3}Gel (Figure 2a, Figure S4, Supporting Information). A similar number and type of aggregates of *S. aureus* formed in a more complex system containing agarose gels.[53] Though, agarose gels have a uniform

© 2023 The Authors. Advanced Functional Materials published by Wiley-VCH GmbH

16163028, 2023, 50, Downloaded from https://advanced.onlinelibrary.wiley.com/doi/10.1002/adfm.202306116 by CochraneItalia, Wiley Online Library on [26/10/2025]. See the Terms and Conditions (https://onlinelibrary.wiley.com/terms-and-conditions) on Wiley Online Library for rules of use; OA articles are governed by the applicable Creative Commons License

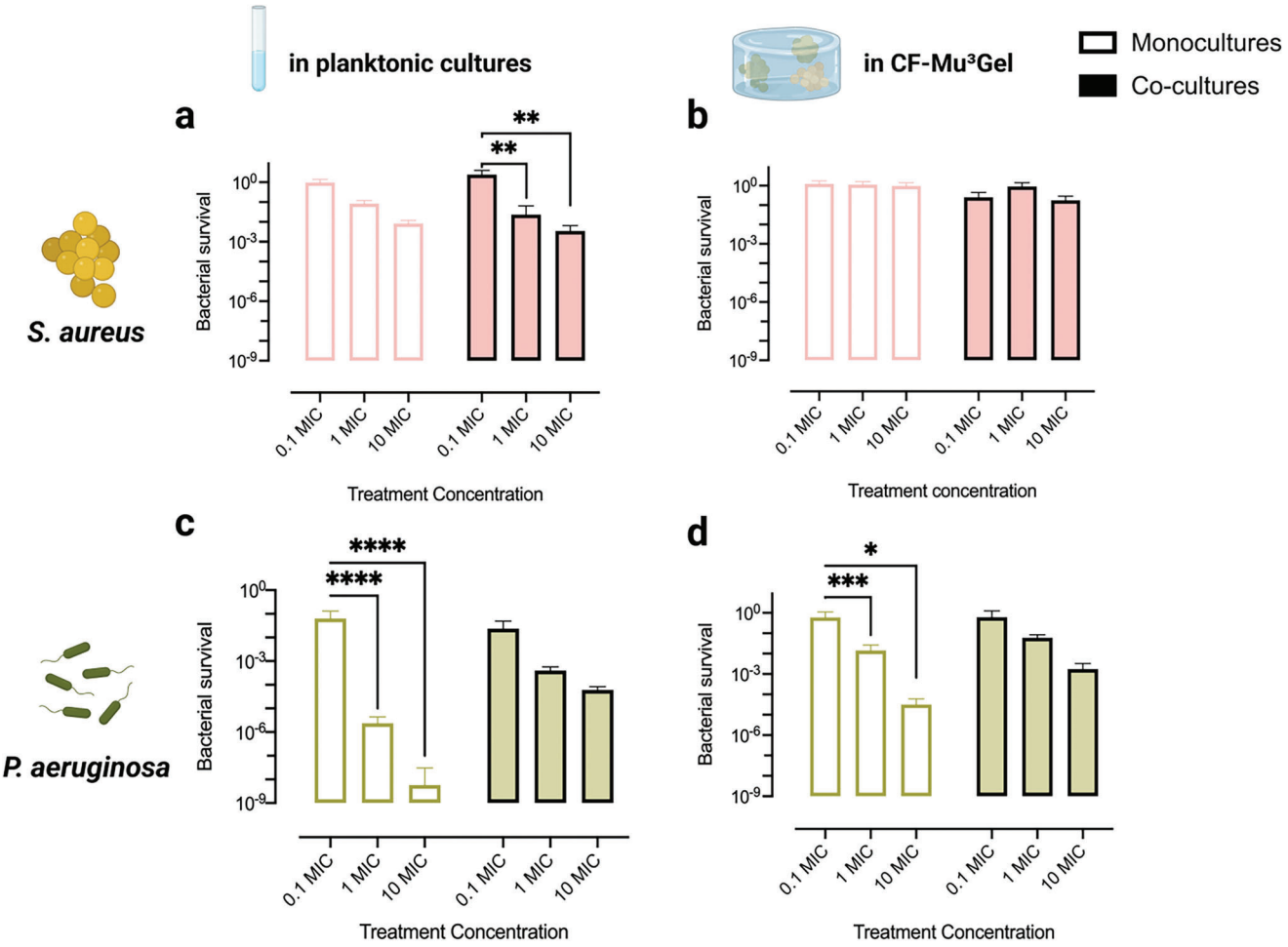

Figure 6. Antimicrobial treatment of CF-Mu^{3}Gel co-colonized with both *S. aureus* and *P. aeruginosa* followed by antimicrobial treatment with ciprofloxacin. 0.1, 1, and 10 MIC correspond to 0.05, 0.5, and 5 mg L^{-1}, respectively. Bacterial survival after ciprofloxacin treatment of mono- (white) and co-cultures (colored) of: a,b) *S. aureus*; and c,d) *P. aeruginosa* either in planktonic conditions (a, c); or CF-Mu^{3}Gel (b, d). Bacterial survival was calculated by dividing the CFU number of *S. aureus* and *P. aeruginosa* after antibiotic treatment by the CFU number of *S. aureus* and *P. aeruginosa* without antibiotic treatment (No ATB). All data were analyzed using two-way ANOVA. Significant differences were set for $*p < 0.05$; $**p < 0.01$; $***p < 0.001$; $****p < 0.0001$. A minimum of five independent samples were analyzed per bacterium ($n \geq 5$).

structure and rely on bacteria O_2 consumption to produce the gradient.[53] Whenever bacteria are introduced in CF-Mu^{3}Gel, they are able to sense, self-organize and exacerbate the O_2 profile (Figure 2d,e), with a higher number of bacteria at the top (Figures S4 and S5, Supporting Information). The heterogeneous structure of CF mucus is not only a natural consequent of mucus build-up, but microbial colonization further contributes to this phenomenon, as, during disease progression, airway CF mucus gradually acquires a heterogeneous structure with detectable O_2 depletion at a few millimeters below the air–mucus interface. Indeed, the resultant O_2 profile reproduces that determined in CF mucus colonized by *S. aureus* and *P. aeruginosa*.[54,55]

Agar or alginate 3D systems such as beads,[56–60] and, more recently, a hydrogel composed of alginate/mucin,[30] have been proposed as suitable means to culture *P. aeruginosa*. The latter is similar to our previous mucus models[61,62] and all of them lack the presence of 3D gradients. Indeed, our results show that bacteria can sense the intrinsic gradients of CF-Mu^{3}Gel. In fact, *P. aeruginosa* forms multicellular aggregates, similar in morphology and size to those seen in CF mucus and chronic wounds (Figure 2b; Figures S5 and S6, Supporting Information).[63,64] The formation of these aggregates is associated with O_2 gradients,[54,65–67] with higher concentration of aggregates at higher O_2 concentrations. This organization leads to increased production of alginate by *P. aeruginosa*,[66,68] a process which is believed to be the underlying cause of chronic infections.[69] This level of organization was also observed in vitro in alginate beads, in which *P. aeruginosa* aggregates were mostly present at the surface.[57,58] Supplementation with NO_3^- promoted the formation of aggregates in deeper layers. In the CF-Mu^{3}Gel, however, there was no need for NO_3^- supplementation to achieve deeper layer colonization and aggregate formation (Figure S5, Supporting Information). Steep O_2 gradients were present in CF-Mu^{3}Gel and anoxia was found after 48 h of culture at 200–300 µm depth with a close similarity to airway CF mucus (Figure 2d,e).[54] These features may be related to the presence of aggregates of both *S. aureus* and *P. aeruginosa*, suggesting possible biofilm formation.[70,71]

© 2023 The Authors. Advanced Functional Materials published by Wiley-VCH GmbH

16163028, 2023, 50, Downloaded from https://advanced.onlinelibrary.wiley.com/doi/10.1002/adfm.202306116 by CochraneItalia, Wiley Online Library on [26/10/2025]. See the Terms and Conditions (https://onlinelibrary.wiley.com/terms-and-conditions) on Wiley Online Library for rules of use; OA articles are governed by the applicable Creative Commons License

16163028, 2023, 50, Downloaded from https://advanced.onlinelibrary.wiley.com/doi/10.1002/adfm.202306116 by CochraneItalia, Wiley Online Library on [26/10/2025]. See the Terms and Conditions (https://onlinelibrary.wiley.com/terms-and-conditions) on Wiley Online Library for rules of use; OA articles are governed by the applicable Creative Commons License

Microbial ecology seems to be highly dependent on the presence of a 3D structure and on the culture period. Different culture conditions have been tested to co-culture *S. aureus* and *P. aeruginosa* in vitro.[8,9,16-22,72-74] Some studies suggest that *P. aeruginosa* outcompetes *S. aureus*,[2,3,6] others refer that *S. aureus* supports colonization and pathogenicity of *P. aeruginosa*[8] or that anaerobiosis is required for their coexistence.[9] In CF-Mu^{3}Gel, both *S. aureus* and *P. aeruginosa* co-existed independently of the experimental condition adopted (Figure 5), while in planktonic conditions, these only co-existed when *S. aureus* was cultured first followed by the addition of *P. aeruginosa* (Figure 5b). Co-cultures under planktonic conditions, by definition, lack a 3D support, meaning that the exoproducts secreted by *P. aeruginosa* and other molecules freely and easily spread in the medium, thus negatively influencing the survival of *S. aureus*. Yet, within a 3D substrate, bacteria by-products slowly diffuse due to interactive and steric phenomena characteristic of 3D environments. This supports the results with CF-Mu^{3}Gel (Figure 5a–c), where both *S. aureus* and *P. aeruginosa* co-exist with a similar number as in the case with CF mucus.[47]

The presence of O_2 gradients may also be a key feature to enable simultaneous growth. It is described that, under anoxia, *S. aureus* growth did not change when co-cultured with either strains or clinical isolates of *P. aeruginosa*.[9] This is further corroborated by our results of mono-cultured *S. aureus* and *P. aeruginosa* that exacerbated the intrinsic O_2 gradients of CF-Mu^{3}Gel with a steep decrease in O_2 tension throughout its thickness (Figure 2d,e). Given that, in CF-Mu^{3}Gel, it was possible to co-culture both bacteria without external apparatus to achieve anaerobic conditions, the proposed 3D substrate provides a further advantage to co-culture these pathogens, and possibly, other complex microbial communities, i.e., polymicrobial infections or microbiota, where it is needed to co-culture anaerobic, microaerophilic and aerobic microorganisms together. In CF-Mu^{3}Gel, both bacteria were able to colonize and form aggregates across the 3D structure, which appear in contact with each other (Figure 5d–f, Figure S9, Supporting Information). When the co-culture period was prolonged from 48 h (Figure 5) to 72 h (Figure S10c, Supporting Information "No ATB"), *P. aeruginosa* progressively overtook *S. aureus*. Indeed, the size of *P. aeruginosa* aggregates increased over longer incubation times, as can be seen in Figure 5e,f, in which *P. aeruginosa* was allowed to grow 24 h in co-culture with pre-cultured of *S. aureus* (*S. aureus* first, followed by another 24 h of co-culture with *P. aeruginosa*), while in the second *P. aeruginosa* was allowed to grow for full 48 h (*P. aeruginosa* first, followed by another 24 h of co-culture with *S. aureus*). The organization of *P. aeruginosa* aggregates (Figure 5e,f) negatively influenced *S. aureus* growth for longer periods of culture (Figure 5b; Figure S10c, Supporting Information "No ATB"). This result is supported by previous studies on the *P. aeruginosa*/*S. aureus* antagonistic phenomenon, in which co-culture induced the secretion of anti-staphylococcal molecules and proteases.[4,5]

It is clearly understood that antimicrobial treatment drastically reduces CF patient's morbidity and increases life expectancy.[75,76] The key therapeutic challenge, however, as addressed in this paper, is that efficacy testing on planktonically cultured bacteria is misleading. Indeed, it is estimated that the antimicrobial tolerance of bacteria in biofilms is 100–1000 times greater than those determined planktonically.[77] With our approach, we reproduced what occurs in CF antimicrobial treatment conditions. This is evidenced by the fact that in the CF-Mu^{3}Gel the number of bacteria after exposure to the minimal inhibitory concentration (MIC) was three orders of magnitude higher than those found under planktonic conditions. Overall, even at antimicrobial concentrations which are lower or higher than the MIC, *S. aureus* and *P. aeruginosa* were more resistant to antimicrobial treatment when cultured within CF-Mu^{3}Gel, independently of the antimicrobial agent (Figure 4a–e). *S. aureus* exhibited high tolerance toward ciprofloxacin, even when shorter incubation periods were adopted, an effect previously linked to reduced ATP levels, associated with inhibition of *S. aureus* respiration by ciprofloxacin.[78] CF-Mu^{3}Gel, as CF mucus, provides a 3D steric and interactive barrier to the diffusion of antimicrobial agents, a phenomenon which may explain the lack of efficiency of antimicrobial treatment (Figure 3). The CF-Mu^{3}Gel, as CF mucus together with the exopolysaccharidic matrix produced by bacteria, offered a significant barrier to the diffusion of all antimicrobial agents (Figure 3 and Figure S7, Supporting Information). The diffusion of colistin sulphate, tobramycin, and ciprofloxacin was strongly reduced by CF-Mu^{3}Gel, possibly due to the interaction of these drugs with mucin,[79] its main component. Colistin and tobramycin are highly positively charged, and as previously demonstrated, these interact with mucins. This binding decreases the MIC potency of antimicrobials.[79]

Low permeability through the mucus may limit the amount of drug that encounters both *S. aureus* and *P. aeruginosa*, thus affecting its efficacy. In this sense, it is significant to note that the MIC of these antimicrobial agents against *S. aureus* and *P. aeruginosa* was shown to be one to three orders of magnitude higher in the presence of mucin.[79,80] The lack of antimicrobial efficiency can be also linked to the formation of persister populations.[81] In CF-Mu^{3}Gel, both *S. aureus* and *P. aeruginosa* were found to be more resistant to ciprofloxacin treatment when co-cultured than when in mono-cultures (Figure 6b,d). This is supported by the literature, as *S. aureus* co-cultured with *P. aeruginosa* revealed to be more resistant to ciprofloxacin treatment when in the presence of one another.[82,83] All of this underscores and emphasizes the need for significantly more reliable screening tools. In the wide library of antimicrobial agents that can be tested, ciprofloxacin, tobramycin and colistin were selected because these are the most administered treatments for CF therapy and because they have distinctive modes of action. Although this suggests that the platform is versatile, we cannot confirm that the observed effects can be extrapolated to other antimicrobial agents. Antimicrobial treatments were performed selecting, as reference concentration, the MIC determined following EUCAST guidelines. However, local concentrations may greatly vary according to the method of administration and the pharmacokinetic of each drug. For example, the local peak concentrations of aerosolized drugs could be different from those determined systematically after oral or intravenous administration.[84-86] The localized presence of mucins may locally negatively affect the antimicrobial efficacy and thus counteract the benefits of local delivery.[79] In fact, by providing the mucin content and the characteristic steric and interactive layers of mucus together with the presence of bacterial aggregates, CF-Mu^{3}Gel closely reproduces the obstacles that antimicrobials must overcome to efficiently treat infections. The obtained results may also suggest that improvement of therapeutic

© 2023 The Authors. Advanced Functional Materials published by Wiley-VCH GmbH

16163028, 2023, 50, Downloaded from https://advanced.onlinelibrary.wiley.com/doi/10.1002/adfm.202306116 by Cochraneltalia, Wiley Online Library on [26/10/2025]. See the Terms and Conditions (https://onlinelibrary.wiley.com/terms-and-conditions) on Wiley Online Library for rules of use; OA articles are governed by the applicable Creative Commons License

strategies against CF airway infections may lay in favoring the diffusion of antimicrobial agents through the CF mucus either by designing antimicrobial drugs that are non-binding to the mucus or by incorporating antimicrobials in micro- to nanoparticles that are able to surpass the mucus barrier. We have in this paper considered the two main pathogens colonizing CF airways and have demonstrated the efficacy of this approach. Further studies are needed to investigate and confirm the ability of CF-Mu^{3}Gel to sustain the growth of multiple pathogens, and possibly the CF airway microbiota retrieved from different patients. Our work has the potential to create opportunities for the development of personalized and effective antimicrobial treatments.

4. Conclusion

In this study, we demonstrate, with this example-based research, the enormous advantage of switching from planktonically cultured bacteria to heterogenous 3D structures that mimic key characteristics of the natural microbial niche, including the presence of O_2 and structural gradients. Specifically, the complex heterogeneity of CF-Mu^{3}Gel enabled single- and dual-species survival and formation of clinically witnessed microcolony aggregates which are characteristic of the CF mucus. These distinctive outcomes were obtained under normal culture conditions, without further use of anaerobic conditions, by simply controlling the materials production, which involved the formation of structural gradients at the molecular level and their characterization. These features required unconventional tools for their characterization, such as PCI. This technique spotted structural and dynamical heterogeneities that can be associated with the gradient of crosslinking produced by the diffusion method.

Considering the possibility to provide a model with a clinical relevance, the proposed mucin-containing hydrogel exhibits a chemical composition, viscoelastic properties and both structural and O_2 gradients that reproduce key features of those of CF airway mucus, but, most importantly, these characteristics drove bacterial organization in size and format similar to those clinically seen in CF mucus. Additionally, the mismatch of 1-to-3 orders of magnitude on the efficacy of antimicrobial treatment between bacteria cultured in traditional methods (planktonic cultures) and those in patients was also depicted in cultures in CF-Mu^{3}Gel. We are aware of the possible limits of the use of commercially available mucins, which are themselves a "model" of the different native mucins within a model. However, the flexibility of the production process does not preclude further tuning of the hydrogel composition to include specific mucins or other components that are relevant to control bacterial behavior.

From a technological point of view, the developed 3D-substrate can be further tuned to closely and accurately model different environmental conditions. This opens the possibility to produce standardized in vitro platforms for basic microbiology research and drug development.

5. Experimental Section

CF-Mu^{3}Gel Properties: Gradient-CF-Mu^{3}Gel (for short, it was termed CF-Mu^{3}Gel) is composed of 2.5% (w/v) porcine stomach type III mucin (Sigma-Aldrich, M1778; lot# SLBQ7188V, Germany) and 0.71% (w/v) sodium chloride that falls within the ranges previously determined in CF sputum.[32,33] G-CF-Mu^{3}Gel was produced in MHB, LB or in 7.07 mg mL^{-1} NaCl. The method of production is now patented (IT102018000020242A).[43] Briefly, G-CF-Mu^{3}Gel was produced using a controlled diffusion system. The apical compartment contained a mucin/alginate solution, while the basolateral compartment comprises the crosslinking media that in this study was composed of different concentrations of Ca^{2+} ions ranging from 0.12–1.20% (w/v). In this way, 3D structures with spatial gradients were generated.

Rheological Characterization: The viscoelastic properties of CF-Mu^{3}Gel produced in different media (7.07 mg mL^{-1} NaCl, MHB, and LB) were evaluated using an Anton Paar MCR502 Rheometer (Austria) with a 25 mm diameter plate geometry (serial number 52530/19910) at 25 °C. The linear viscoelastic region (LVR) was determined through strain sweep analyses employing a strain logarithmic ramp varying from 0.1% to 1000% at a frequency of 1 Hz. Oscillatory frequency sweeps were further performed to evaluate both storage, G', and dissipative, G'', moduli, as well as complex shear modulus, G^*, at 0.5% (at strain amplitudes within the linear regime) with frequencies changing logarithmically in the 0.1–20 Hz range. The viscoelastic properties of CF-Mu^{3}Gel were further compared to those reported for CF sputum. A detailed analysis was conducted at the characteristic frequencies of breathing (0.5 Hz) and ciliary beating (10 Hz) under physiologic conditions.[34-36] The rheological data was further exploited to estimate the mesh size of different formulations of CF-Mu^{3}Gel by exploiting both the generalized Maxwell model and the rubber elasticity theory, as previously reported.[43,61]

Photon Correlation Imaging (PCI): PCI is an optical technique that blends the power of Dynamic Light Scattering (DLS) with that of digital imaging. The setup employed for the characterization of CF-Mu^{3}Gel is reported in Figure S2 (Supporting Information), adapted from a previous setup.[87] A classical DLS experiment allows one to investigate the microscopic dynamics of a sample by measuring the degree of correlation c(t, t+τ) between the intensity of the light scattered by the sample at two different times t and t+τ. In the simplest case of the Brownian motion of a dispersed nanoparticle, for instance, this quantity is simply related to particle diffusion over distances of the order of the inverse of the scattered wave vector $q = 4\pi/\lambda \sin(\theta/2)$, where θ is the angle at which the scattered light is measured (in the experiment, $\theta = 90°$) and is the wavelength of the scattered light. PCI yields similar information but, by operating on an image of the sample produced on a CMOS multi-pixel camera by a suitable "stopped-down" optics,[88] retains at the same time the spatial resolution of an imaging system. This allows the spatial distribution of both the scattered intensity and of the degree of correlation at the given delay time t to be mapped (respectively dubbed "intensity" and "correlation" maps). To the aims, PCI has two main advantages with respect to standard DLS:

(a) it provides spatial distribution of both the scattered intensity and of the degree of correlation, thus allowing to spot and quantify heterogeneity both in the structure and in the microscopic dynamics of the sample.

(b) standard DLS measurements require the medium to be "ergodic," namely that the scatterers are free to move over distances that are not much smaller than the wavelength. This condition, which is required for the averages in time measured in a DLS experiment to coincide with true statistical averages ("ensemble" averages), is satisfied by Brownian particle dispersions, but not by a hydrogel, where the microscopic motion is almost completely frozen. This limitation is overcome by PCI, where a correct ensemble average is easily obtained from a spatial average over a suitable but still "region of interest." Thus, PCI provides a unique method to investigate the slow and spatially limited spontaneous restructuring dynamics of soft disordered solids.[88]

Bacterial Strains and Culture Conditions: The microorganisms used were *Staphylococcus aureus* ATCC 25923 (*S. aureus*) and *Pseudomonas aeruginosa* ATCC 15692 (PA01 strain, *P. aeruginosa*), kindly supplied by R. Migliavacca (Department of Clinical Surgical, Diagnostic and

© 2023 The Authors. Advanced Functional Materials published by Wiley-VCH GmbH

16163028, 2023, 50, Downloaded from https://advanced.onlinelibrary.wiley.com/doi/10.1002/adfm.202306116 by CochraneItalia, Wiley Online Library on [26/10/2025]. See the Terms and Conditions (https://onlinelibrary.wiley.com/terms-and-conditions) on Wiley Online Library for rules of use; OA articles are governed by the applicable Creative Commons License

Paediatric Sciences, University of Pavia, Italy). Brain heart infusion broth (BHI; Sigma-Aldrich, 53286, Germany) and Luria Bertani broth (LB; Formedium, LMM0102, United Kingdom) were used to inoculate *S. aureus* and *P. aeruginosa*, respectively. Bacteria were grown overnight in their appropriate medium, under aerobic conditions at 37 °C using a shaker incubator (VDRL Stirrer 711/CT, Asal Srl, Italy). Both cultures were prepared at the final density of 1×10^9 bacteria mL^{-1} as determined by comparing the optical density at 600 nm (OD600) of the sample with a standard curve relating OD600 to bacterial number by using a UV-VIS spectrophotometer (Aurogene S.r.l., HJ1908003, Italy).[89] Müller Hinton broth (MHB; Sigma-Aldrich, 70192, Germany) was used to prepare the final inoculum of both bacterial mono- and co-cultures to be inoculated in CF-Mu^{3}Gel or used as planktonic culture controls. The total number of colony forming units (CFU) was counted by plating the serial dilutions (prepared in 0.9% NaCl) of bacterial cultures on Müller Hinton agar (MH agar; Sigma-Aldrich, 70191, Germany) plates, while cetrimide agar (Sigma-Aldrich, 22470, Germany) and mannitol salt (Sigma-Aldrich, 63567, Germany) were used as selective media to count the CFU of *P. aeruginosa* and *S. aureus* after co-culture experiments, respectively. All media and plates of MH, mannitol salt and cetrimide agar were prepared following supplier instructions. Sodium citrate tribasic dihydrate (NaCitrate; Sigma-Aldrich, 71404, Germany) was used as a dissolving agent of CF-Mu^{3}Gel to retrieve bacteria that grew within its 3D structure. Three antimicrobial agents were used, including colistin (Sigma-Aldrich, C4461, Germany), ciprofloxacin (Fresenius Kabi, lot# 15LA518P2, Italy), and tobramycin (Ibi, lot# 118B, Italy).

Mono-Cultures in CF-Mu^{3}Gel: *S. aureus* or *P. aeruginosa* were cultured in CF-Mu^{3}Gel for 24 and 48 h incubation. After overnight culture, the bacterial suspension was subsequently diluted in fresh medium, until reaching the final concentration of 10^4 bacterial cells mL^{-1}. Cultures in CF-Mu^{3}Gel were achieved by inoculating on the top 100 µL of each separated bacterial suspension and incubating for 24 and 48 h at 37 °C. Planktonic cultures of *S. aureus* or *P. aeruginosa* (i.e., bacteria cultured in liquid medium without hydrogels) in 96 multiwell flat tissue culture plates were used as controls of the experiment.

Co-Cultures in CF-Mu^{3}Gel: Co-cultures of both *S. aureus* and *P. aeruginosa* were induced in CF-Mu^{3}Gel in a proportion of 1:1 following three different co-culture settings: a) simultaneous culture of both *P. aeruginosa* and *S. aureus* for 24 h; b) culturing first *S. aureus* for 24 h followed by *P. aeruginosa* cultured for another 24 h; and finally, c) colonizing CF-Mu^{3}Gel with *P. aeruginosa* first for 24 h, after which *S. aureus* was added and incubated for further 24 h. Before adding the second bacterial strain, the excess medium was removed and substituted with 100 µL of 10^4 bacterial cells mL^{-1} of the secondly introduced bacterium. Co-cultures of *S. aureus* and *P. aeruginosa* in planktonic conditions were also carried out as the controls of the experiment for the three different co-culture settings.

Bacterial Viability within CF-Mu^{3}Gel: CF-Mu^{3}Gel was dissolved with 150 µL of 50 mM NaCitrate, pH 7.4, for bacterial viability determination. After 2 min contact time, the suspension was diluted to 10^{-6}–10^{-10} in 0.9% NaCl solution, pH 7.4, to perform serial dilution and CFU counting. MH agar plates were incubated overnight at 37 °C. When co-cultures were carried out, the total number of CFU was counted using MH agar plates, while cetrimide or mannitol salt agar plates were used as selective media to count the CFU of *P. aeruginosa and S. aureus*, respectively. CFUs were then calculated taking into consideration a dilution factor of 2.5, resulting from the addition of 50 mM sodium citrate. Planktonic cultures of *S. aureus* or *P. aeruginosa* were used as controls of the experiment.

Oxygen Tension Measurements: O_2 tension of colonized CF-Mu^{3}Gel was measured using a Clark-type O_2 sensor (OX-25; Unisense, Aarhus N, Denmark), connected to the Unisense microsensor multimeter S/N 8678 (Unisense, Denmark), a high sensitivity pico-ampere four-channel amplifier. Before each measurement, the reference anode and the guard cathode were polarized overnight and calibrated with either water saturated with air or with an anoxic solution of 2% (w/w) sodium hydrosulfite. Once the calibration was carefully made, a low melting point agarose consisting of 2% (w/v) agarose in 0.071% (w/v) NaCl (same concentration as in CF-Mu^{3}Gel) was cast into a petri dish. CF-Mu^{3}Gel colonized with either *S. aureus* or *P. aeruginosa* were placed over the agarose layer. Microsensors with a tip diameter of 50 µm (OX-50) were positioned at the air–CF-Mu^{3}Gel interface ("depth zero") using a motorized micromanipulator (Unisense, Denmark). Measurements were performed at the center of the hydrogels starting at their surface (0 mm) through their thickness, every 100 µm in triplicate, until the tip completely penetrated the whole structure. The maximum depth reached by the tip, termed end depth, was 2300 µm. Sterile CF-Mu^{3}Gel was used as control of the experiment. The Unisense software SensorTrace automatically converts the signal from partial pressure (O_2 tension) to the equivalent O_2 concentration in µmol L^{-1}.

Bacterial Colonization within CF-Mu^{3}Gel: *Preparation of the DsRed-fluorescent strain of S. aureus ATCC 25923*: To obtain a DsRed-fluorescent strain, *S. aureus* ATCC 25923 was transformed by electroporation with the pCAG-DsRed plasmid DNA following the protocol suggested by Schenk and Laddaga (1992).[90] Chloramphenicol (CP) was used at 10 µg mL^{-1} (Sigma-Aldrich, Germany). pCAG-DsRed was a gift from Connie Cepko (Addgene plasmid #11151; http://n2t.net/addgene:11151; RRID:Addgene_11151). Plasmid manipulation was performed according to standard techniques.

Preparation of the GFP-fluorescent strain of P. aeruginosa PA01: To obtain a GFP-fluorescent strain, *P. aeruginosa* PA01 was transformed by electroporation with the pMF230 plasmid DNA following the protocol reported by Cadoret et al. (2014).[91] Carbenicillin (CB) was used at 300 µg mL^{-1}. pMF230 was a gift from Michael Franklin (Addgene plasmid #62546; http://n2t.net/addgene:62546; RRID:Addgene_62546). Plasmid manipulation was performed according to standard techniques.

Mono-Cultures in CF-Mu^{3}Gel: The viability of *S. aureus* ATCC 25923 or *P. aeruginosa* PA01 within CF-Mu^{3}Gel was assessed using the Live/Dead dual staining BacLight Kit (Live/Dead Bacterial Viability Kit, L-7007, Molecular Probes) according to manufacturer specifications. The BacLight kit is composed of two fluorophores SYTO9 and propidium iodide (PI) that stain total and dead bacteria, respectively. After 10 min incubation with SYTO9, the colonized CF-Mu^{3}Gel was washed three times, followed by a 3 min staining with PI. Viable (green) and non-viable (red) bacteria within CF-Mu^{3}Gel were differentiated by using the dual-channel option of the Leica TCS SP8 confocal microscope. Since the *P. aeruginosa* strain fluoresces green, only the PI or Hoechst 33342 (Hoechst; Invitrogen, Eugene, Code) staining were used, whereas for *S. aureus* (fluoresces in red) only the SYTO9 was used.

Co-Cultures in CF-Mu^{3}Gel: The experiment was performed using DsRed-*S. aureus* ATCC 25923 (red fluorescence) and GFP-*P. aeruginosa* PA01 (green fluorescence) to discriminate between the two bacterial strains. The general total number of these bacteria after co-culture in CF-Mu^{3}Gel was evaluated using the Hoechst 33342 staining. Hoechst 33342 can readily cross cell membranes to stain the DNA (blue) of total bacteria (blue). 50 µL of a mixture of Hoechst 33342 with a final concentration of 1 µg mL^{-1} was added to each colonized CF-Mu^{3}Gel. After Hoechst staining, DsRed-*S. aureus* ATCC 25923 appeared purple and the GFP-*P. aeruginosa* PA01 were blue-green.

Confocal Laser Scanning Microscopy: CF-Mu^{3}Gel were seeded with DsRed-expressing *S. aureus* and/or GFP-expressing *P. aeruginosa* to analyze bacterial colonization in mono- and co-cultures using Confocal Laser Scanning Microscopy. In this way, cultures were performed in CF-Mu^{3}Gel following the aforementioned method to induce mono- and co-cultures for 12, 24, and 48 h. After each incubation period, colonized CF-Mu^{3}Gel were observed under a high-resolution spectral confocal-laser microscope (Leica TCS SP8 SMD, Leica Microsystems CMS GmbH, Germany). Colonized CF-Mu^{3}Gel were analyzed from the top, bottom, and middle. Analyses were performed at different wavelengths according to fluorochrome and staining, namely 550 (570/650) nm excitation for DsRed-expressing *S. aureus*, 488 (500/550) nm excitation for both GFP-expressing *P. aeruginosa* and SYTO9, 535 (570/670) nm excitation for PI, and 405 (420/500) nm excitation for Hoechst 33342. The 3D images obtained were analyzed using the LasX 3.7.5 software provided by Leica. In the case of monocultures by DsRed-*S. aureus* ATCC 25923, CF-Mu^{3}Gel was supplemented with 10 µg mL^{-1} CP, whereas in the case of mono-cultures by GFP-expressing *P. aeruginosa* PA01, CF-Mu^{3}Gel containing 300 µg mL^{-1} CB

© 2023 The Authors. Advanced Functional Materials published by Wiley-VCH GmbH

was used. As a control, CF-Mu^{3}Gel without bacteria was observed under confocal microscopy at the aforementioned wavelengths to evaluate the absence of possible autofluorescence effects.

Antimicrobial Susceptibility: Determination of Minimal Inhibitory Concentration: Ciprofloxacin, tobramycin, and colistin were selected as antimicrobial agents to which *P. aeruginosa* is sensitive to determine antimicrobial susceptibility within CF-Mu^{3}Gel, while ciprofloxacin chosen as antimicrobial agents against *S. aureus*. The minimal inhibitory concentration (MIC) was determined by the broth microdilution method using MHB inoculated with a standard inoculum according to The European Committee on Antimicrobial Susceptibility Testing (EUCAST) guidelines. In this way, 10^3 bacterial cells in MHB were incubated with serial dilutions of 1:2 of each antimicrobial agent (0, 0.0625, 0.125, 0.25, 0.5, 1, 2, 4, 8, 16, 32, 64 mg L^{-1}) for 24 h at 37 °C. OD600 was measured to determine the values of MIC using the 3-(4,5-Dimethylthiazol-2-yl)-2,5-Diphenyltetrazolium Bromide (MTT) colorimetric test (Sigma-Aldrich, Germany) according to supplier instructions, which transforms the metabolic products of bacteria into a violet observable precipitate that can be read using a spectrophotometer. The intensity of the violet color is proportional to the number of viable bacteria. The plate was then read at a wavelength of 570 nm and the background read at 630 nm was subtracted (Clariostar microplate reader, BMG Labtech Clariostar, Germany). MIC was established as the lowest concentration of antimicrobial agents that inhibited bacterial growth.

Antimicrobial Susceptibility within CF-Mu^{3}Gel: Mono-cultures of either *S. aureus* or *P. aeruginosa* in CF-Mu^{3}Gel were induced by culturing 10^3 bacteria to achieve 10^8 bacteria after 24 h of culture. After this period, the supernatant over the hydrogels was removed and these were washed twice with fresh MHB medium. Then, 100 µL of antimicrobial agent at three different concentrations was added, namely 0.1, 1, and 10 MIC. Antimicrobial treatment was carried out for 24 h under static incubation, at 37 °C, after which CFU count was performed. Similarly, co-cultures of *P. aeruginosa* and *S. aureus* in CF-Mu^{3}Gel were treated with ciprofloxacin, given that both bacteria are sensitive to this antimicrobial agent. Both *S. aureus* and *P. aeruginosa* were cultured in CF-Mu^{3}Gel in a proportion of 1:1 following the co-culture setting b: culturing *S. aureus* first followed by *P. aeruginosa* cultured for another 24 h. Several controls were performed: I) planktonic cultures after antimicrobial treatment; II) planktonic cultures without antimicrobial treatment; and III) non-treated but colonized CF-Mu^{3}Gel. Both MHB medium and CF-Mu^{3}Gel without bacteria and antimicrobial treatment were used as controls of sterility.

Drug Diffusion Studies: Drug diffusion studies were conducted using either polycarbonate Transwell supports (Corning Transwell, CLS3413, Merck) with a porosity of 0.4 µm and inner diameter equal to 6.5 mm or a 96-well plate permeable support system with a filter plate pre-coated with structured layers of phospholipids (PAMPA; Corning Gentest Pre-coated PAMPA, 353015, USA) with a porosity of 0.45 µm and inner diameter equal to 6.2 mm. Drug diffusion through empty Transwell inserts and empty PAMPA were performed as controls of the experiment. Both ciprofloxacin, tobramycin, and colistin were tested at a concentration of 500 µM. CF-Mu^{3}Gel was introduced on both platforms with a thickness of ≈500 µm. Afterward, the donor compartment was filled with the relevant drug solution (200 µL per well) and 300 µL of phosphate saline buffer was added to the acceptor compartment. The filter plate was then coupled to the receiver plate and incubated at room temperature without agitation for 5 and 24 h. At the end of the incubation period, the plates were separated and the volume of both the donor and the receiver plate was collected for further quantification. Liquid chromatography-mass spectrometry was further carried out to quantify the permeated amount of drugs using their relevant calibration curves. The percentage of drug permeated after 5 and 24 h was calculated as follows:

$$\%\ \text{drug permeated} = \frac{C_t}{C_0} \times 100 \quad (1)$$

where C_t denotes the concentration of drug released at time t, and C_0 represents the initial concentration introduced on the donor compartment. The apparent permeability coefficient (P_{app}) was expressed using Equation (1) derived from Fick's law[92] for steady state conditions:

$$P_{app} = \frac{dQ/dt}{C_0 \times A} \quad (2)$$

where dQ is the quantity of drug expressed as moles permeated into the acceptor compartment at time t (18 000 s), C_0 is the initial concentration in the donor well, and A is the area of the well membrane (0.3 cm^2). The P_{app} was used as an average of all the measures.

Liquid Chromatography–Mass Spectroscopy: An HPLC-MS using a Varian HPLC equipped with a 410 autosampler and an Ascentis C18 column (10 cm × 2.1 mm, 3 µm). Gradient mobile phases composed of acetonitrile and water with 0.1% formic acid as organic and aqueous phases, respectively, were pumped at a flow rate of 200 µL min^{-1}. A flow of 200 µL min^{-1} and an injection volume of 10 µL were used. Compounds were detected on a Varian 320 MS TQ Mass Spectrometer equipped with an electrospray ionization (ESI) source operating in positive mode. The detector was used in multiple reaction monitoring (MRM) mode and the transitions of each drug are reported in Table S1 (Supporting Information).

Statistical Analysis: The results of at least three independent experiments are presented as mean ± standard deviation (SD). Statistical analysis was performed using the *t*-test student and ANOVA using GraphPad Prism version 8 (GraphPad Software, USA). Significant differences were set for $*p < 0.05$. *n* corresponds to the number of distinct samples in which different measurements were performed.

Supporting Information

Supporting Information is available from the Wiley Online Library or from the author.

Acknowledgements

D.P.P and P.P. would like to thank Switch2Product (UA.A.RRR.ARICID.SVRA.AUTO.AZ18VARI10) for partially funding the validation of the technology to be employed as airway models. This work was also supported by two grants of the Italian Ministry of Education, University and Research (MIUR) to Politecnico di Milano MIUR PRIN 2017 "Soft Adaptive Networks" and the Department of Molecular Medicine of the University of Pavia under the initiative "Dipartimenti di Eccellenza (2018–2022 and 2023-2027)." The authors are grateful to P. Vaghi (Centro Grandi Strumenti https://cgs.unipv.it/eng/, University of Pavia, Pavia, Italy) for her technical assistance during CLSM analysis. A special thanks to Scott Burgess (University of Pavia, Pavia, Italy) for correcting the English in the manuscript. The authors would like to thank Annalisa Balloi, Politecnico di Milano, for the productive discussion and suggestions. The schematic representations included in the manuscript were created with BioRender.com.

Conflict of Interest

The authors declare no conflict of interests. D.P.P., F.B., N.S.V., S.V., L.V., and P.P. are co-inventors of the patented technology. D.P.P. is co-founder, shareholder, and CTO of Bac3Gel, Lda, a mucus-based company. S.v.U. is co-founder, shareholder, and CEO of Bac3Gel, Lda. S.V., L.V., and P.P. are co-founders, shareholders, and scientific advisors of Bac3Gel, Lda. The patented technology reported in this study is now exclusively licensed to Bac3Gel startup, which now produces CF-Mu^{3}Gel.

Author Contributions

The multidisciplinary approach and collaborations established in this work were managed by P.P. with the conceptualization and direction of the study

© 2023 The Authors. Advanced Functional Materials published by Wiley-VCH GmbH

16163028, 2023, 50, Downloaded from https://advanced.onlinelibrary.wiley.com/doi/10.1002/adfm.202306116 by CochraneItalia, Wiley Online Library on [26/10/2025]. See the Terms and Conditions (https://onlinelibrary.wiley.com/terms-and-conditions) on Wiley Online Library for rules of use; OA articles are governed by the applicable Creative Commons License

supported by S.V. and L.V., which equally contributed to the manuscript. D.P.P. and N.S.V. developed the production method of CF-Mu^{3}Gel, under the supervision of P.P. D.P.P., F.B., N.S.V., G.G. and A.Z. established and conducted the microbiological and antimicrobial susceptibility analyses under the supervision of LV. D.P.P., A.Z., G.G., and S.v.U. carried out confocal microscopic investigations and analyses. C.S.B. determined the permeability of the antimicrobial agents under the supervision of S.V. D.P.P. performed the rheological characterization and further analyses of all variations of CF-Mu^{3}Gel under the supervision of F.B.V. D.P.P. and E.C. established and performed the analyses of O_2 tension. D.P.P., S.v.U. prepared the samples for PCI analysis. V.R., S.B analyzed PCI data under the supervision of R.P. D.P.P. wrote the original draft of the manuscript and took care of the revisions of the draft, P.P. contributed to the writing and revisions. All authors discussed the results, reviewed the manuscript, and contributed to its final version.

Data Availability Statement

The data that support the findings of this study are available from the corresponding author upon reasonable request.

Keywords

3D cultures, gradients, microbial cultures, microbial ecology

Received: May 31, 2023
Revised: July 21, 2023
Published online: August 22, 2023

[1] J. Jo, A. Price-Whelan, L. E. P. Dietrich, *Nat. Rev. Microbiol.* **2022**, *20*, 593.
[2] C. F. Michelsen, A. J. Christensen, S. Bojer, N. Høiby, H. Ingmer, *J. Bacteriol.* **2014**, *196*, 3903.
[3] R. Baldan, C. Cigana, F. Testa, I. Bianconi, M. De Simone, D. Pellin, C. Di Serio, A. Bragonzi, D. M. Cirillo, *PLoS One* **2014**, *9*, e89614.
[4] J. V. Fahy, B. F. Dickey, *N. Engl. J. Med.* **2010**, *363*, 2233.
[5] A. Hotterbeekx, S. Kumar-Singh, H. Goossens, S. Malhotra-Kumar, *Front. Cell. Infect. Microbiol.* **2017**, *7*, 1023.
[6] L. M. Filkins, J. A. Graber, D. G. Olson, E. L. Dolben, L. R. Lynd, S. Bhuju, A. O. Toole, *J. Bacteriol.* **2015**, *197*, 2252.
[7] J. Haaber, M. T. Cohn, D. Frees, T. J. Andersen, H. Ingmer, *PLoS One* **2012**, *7*, e41075.
[8] P. M. Alves, E. Al-Badi, C. Withycombe, P. M. Jones, K. J. Purdy, S. E. Maddocks, *Pathog. Dis.* **2018**, *76*, 003.
[9] R. Pallett, L. J. Leslie, P. A. Lambert, I. Milic, A. Devitt, L. J. Marshall, *Sci. Rep.* **2019**, *9*, 6748.
[10] T.-F. C. Mah, G. A. O'Toole, *Trends Microbiol.* **2001**, *9*, 34.
[11] D. P. Pacheco, N. Suárez Vargas, S. Visentin, P. Petrini, *Biomater. Sci.* **2021**, *9*, 70.
[12] M. Oriano, L. Zorzetto, G. Guagliano, F. Bertoglio, S. van Uden, L. Visai, P. Petrini, *Front. Bioeng. Biotechnol.* **2020**, *8*, 539319.
[13] J. Huang, S. Liu, C. Zhang, X. Wang, J. Pu, F. Ba, S. Xue, H. Ye, T. Zhao, K. Li, Y. Wang, J. Zhang, L. Wang, C. Fan, T. K. Lu, C. Zhong, *Nat. Chem. Biol.* **2019**, *15*, 34.
[14] S. Balasubramanian, M. E. Aubin-Tam, A. S. Meyer, *ACS Synth. Biol.* **2019**, *8*, 1564.
[15] M. del Mar Cendra, N. Blanco-Cabra, L. Pedraz, E. Torrents, *Sci. Rep.* **2019**, *9*, 16284.
[16] D. H. Limoli, G. B. Whitfield, T. Kitao, M. L. Ivey, M. R. Davis, N. Grahl, D. A. Hogan, L. G. Rahme, P. L. Howell, G. A. O'Toole, J. B. Goldberg, *mBio* **2017**, *8*, e00186.
[17] L. Camus, P. Briaud, S. Bastien, S. Elsen, A. Doléans-Jordheim, F. Vandenesch, K. Moreau, *ISME J.* **2020**, *14*, 3093.
[18] E. Y. Trizna, M. N. Yarullina, D. R. Baidamshina, A. V. Mironova, F. S. Akhatova, E. V. Rozhina, R. F. Fakhrullin, A. M. Khabibrakhmanova, A. R. Kurbangalieva, M. I. Bogachev, A. R. Kayumov, *Sci. Rep.* **2020**, *10*, 8475.
[19] J. R. Lenhard, N. M. Smith, C. D. Quach, T. Q. Nguyen, L. H. Doan, J. Chau, *J. Antimicrob. Chemother.* **2019**, *74*, 2657.
[20] M. Tognon, T. Köhler, A. Luscher, C. Van Delden, *BMC Genomics* **2019**, *20*, 30.
[21] M. Tognon, T. Köhler, B. G. Gdaniec, Y. Hao, J. S. Lam, M. Beaume, A. Luscher, A. Buckling, C. Van Delden, *ISME J.* **2017**, *11*, 2233.
[22] T. Samad, N. Billings, A. Birjiniuk, T. Crouzier, P. S. Doyle, K. Ribbeck, *ISME J.* **2017**, *11*, 1933.
[23] E. Pernet, L. Guillemot, P. R. Burgel, C. Martin, G. Lambeau, I. Sermet-Gaudelus, D. Sands, D. Leduc, P. C. Morand, L. Jeammet, M. Chignard, Y. Wu, L. Touqui, *Nat. Commun.* **2014**, *5*, 5105.
[24] P. Briaud, S. Bastien, L. Camus, M. Boyadjian, P. Reix, C. Mainguy, F. Vandenesch, A. Doléans-Jordheim, K. Moreau, *Front. Cell. Infect. Microbiol.* **2020**, *10*, 266.
[25] G. Orazi, G. A. O'Toole, *mBio* **2017**, *8*, e00873.
[26] A. Moretta, C. Scieuzo, A. M. Petrone, R. Salvia, M. D. Manniello, A. Franco, D. Lucchetti, A. Vassallo, H. Vogel, A. Sgambato, P. Falabella, *Front. Cell. Infect. Microbiol.* **2021**, *11*, 668632.
[27] M. E. V. Johansson, G. C. Hansson, *Nat. Rev. Immunol.* **2016**, *16*, 639.
[28] H. Yan, M. Melin, K. Jiang, M. Trossbach, B. Badadamath, K. Langer, B. Winkeljann, O. Lieleg, J. Hong, H. N. Joensson, T. Crouzier, *Adv. Funct. Mater.* **2021**, *31*, 2105967.
[29] X. Jin, F. B. Yu, J. Yan, A. M. Weakley, V. Dubinkina, X. Meng, K. S. Pollard, *Nat. Commun.* **2023**, *14*, 3510.
[30] A. J. Huang, C. L. O'Brien, N. Dawe, A. Tahir, A. J. Scott, B. M. Leung, *Sci. Rep.* **2022**, *12*, 5515.
[31] M. Quintana-Hayashi, M. Padra, J. Padra, J. Benktander, S. Lindén, *Microorganisms* **2018**, *6*, 55.
[32] M. O. Henke, G. John, M. Germann, H. Lindemann, B. K. Rubin, *Am. J. Respir. Crit. Care Med.* **2007**, *175*, 816.
[33] H. Matsui, B. R. Grubb, R. Tarran, S. H. Randell, J. T. Gatzy, C. W. Davis, R. C. Boucher, *Cell* **1998**, *95*, 1005.
[34] S. Lum, P. Gustafsson, H. Ljungberg, G. Hu, A. Bush, B. Carr, R. Castle, A. Hoo, J. Price, S. Ranganathan, J. Stroobant, A. Wade, C. Wallis, H. Wyatt, J. Stocks, *Thorax* **2007**, *62*, 341.
[35] H. Wilkens, B. Weingard, A. Lo Mauro, E. Schena, A. Pedotti, G. W. Sybrecht, A. Aliverti, A. Aliverti, *Thorax* **2010**, *65*, 808.
[36] D. B. Hill, P. A. Vasquez, J. Mellnik, S. A. Mckinley, A. Vose, F. Mu, A. G. Henderson, S. H. Donaldson, N. E. Alexis, R. C. Boucher, M. G. Forest, *PLoS One* **2014**, *9*, e87681.
[37] S. Yuan, M. Hollinger, M. E. Lachowicz-scroggins, S. C. Kerr, E. M. Dunican, B. M. Daniel, S. Ghosh, S. C. Erzurum, B. Willard, S. L. Hazen, X. Huang, S. D. Carrington, S. Oscarson, J. V. Fahy, *Sci. Transl. Med.* **2015**, *7*, 276ra27.
[38] J. S. Suk, S. K. Lai, Y. Y. Wang, L. M. Ensign, P. L. Zeitlin, M. P. Boyle, J. Hanes, *Biomaterials* **2009**, *30*, 2591.
[39] M. Stigliani, M. D. Manniello, O. Zegarra-Moran, L. Galietta, L. Minicucci, R. Casciaro, E. Garofalo, L. Incarnato, R. P. Aquino, P. Del Gaudio, P. Russo, *J. Aerosol Med. Pulm. Drug Delivery* **2016**, *29*, 337.
[40] P. G. Bhat, D. R. Flanagan, M. D. Donovan, *J. Pharm. Sci.* **1996**, *85*, 624.
[41] H. Nielsen, S. Hvidt, C. A. Sheils, P. A. Janmey, *Biophys. Chem.* **2004**, *112*, 193.
[42] D. D. Sriramulu, H. Lu, J. S. Lam, U. Romling, *J. Med. Microbiol.* **2005**, *54*, 667.

© 2023 The Authors. Advanced Functional Materials published by Wiley-VCH GmbH

16163028, 2023, 50, Downloaded from https://advanced.onlinelibrary.wiley.com/doi/10.1002/adfm.202306116 by CochraneItalia, Wiley Online Library on [26/10/2025]. See the Terms and Conditions (https://onlinelibrary.wiley.com/terms-and-conditions) on Wiley Online Library for rules of use; OA articles are governed by the applicable Creative Commons License

[43] L. Pedersoli, S. Zhang, F. Briatico-Vangosa, P. Petrini, R. Cardinaels, J. Toonder, D. P. Pacheco, *Biotechnol. Bioeng.* **2021**, *118*, 3898.
[44] E. Secchi, F. Munarin, M. D. Alaimo, S. Bosisio, S. Buzzaccaro, G. Ciccarella, V. Vergaro, P. Petrini, R. Piazza, *J. Phys.: Condens. Matter* **2014**, *26*, 464106.
[45] T. Wong, M. C. Roberts, L. Owens, F. M., S. A. L., *J. Med. Microbiol.* **1984**, *17*, 113.
[46] A. C. Jacobsen, S. Visentin, C. Butnarasu, P. C. Stein, M. P. di Cagno, *Pharmaceutics* **2023**, *15*, 592.
[47] A. J. Fischer, S. B. Singh, M. M. LaMarche, L. J. Maakestad, Z. E. Kienenberger, T. A. Peña, D. A. Stoltz, D. H. Limoli, *Am. J. Respir. Crit. Care Med.* **2021**, *203*, 328.
[48] H. G. Ahlgren, A. Benedetti, J. S. Landry, J. Bernier, E. Matouk, D. Radzioch, L. C. Lands, S. Rousseau, D. Nguyen, *BMC Pulm. Med.* **2015**, *15*, 67.
[49] M. O. Henke, A. Renner, R. M. Huber, M. C. Seeds, B. K. Rubin, *Am. J. Respir. Cell Mol. Biol.* **2004**, *31*, 86.
[50] T. Bjarnsholt, *APMIS* **2013**, *136*, 1.
[51] L. Sardelli, D. Pacheco, L. Zorzetto, C. Rinoldi, W. Święszkowski, P. Petrini, *J. Appl. Biomater. Funct. Mater.* **2019**, *17*, 228080001982902.
[52] P. Demianenko, B. Minisini, M. Lamrani, F. Poncin-Epaillard, *Polym. Test.* **2016**, *53*, 299.
[53] B. Pabst, B. Pitts, E. Lauchnor, P. S. Stewart, *Antimicrob. Agents Chemother.* **2016**, *60*, 6294.
[54] E. S. Cowley, S. H. Kopf, A. Lariviere, W. Ziebis, D. K. Newman, *mBio* **2015**, *6*, e00767.
[55] M. Kolpen, M. Kühl, T. Bjarnsholt, C. Moser, C. R. Hansen, L. Liengaard, A. Kharazmi, T. Pressler, N. Høiby, P. Ø. Jensen, *PLoS One* **2014**, *9*, e84353.
[56] B. G. S. Torres, R. Awad, S. Marchand, W. Couet, F. Tewes, *Eur. J. Pharm. Biopharm.* **2019**, *143*, 35.
[57] B. Cao, L. Christophersen, K. Thomsen, M. Sønderholm, T. Bjarnsholt, P. Ø. Jensen, N. Høiby, C. Moser, *J. Antimicrob. Chemother.* **2015**, *70*, 2057.
[58] M. Sønderholm, K. N. Kragh, K. Koren, T. H. Jakobsen, S. E. Darch, M. Alhede, P. Ø. Jensen, M. Whiteley, M. Kühl, T. Bjarnsholt, *Appl. Environ. Microbiol.* **2017**, *83*, e00113.
[59] S. Stenvang Pedersen, G. H. Shand, B. Langvad Hansen, G. Norgaard Hansen, *APMIS* **1990**, *98*, 203.
[60] L. Christophersen, F. A. Schwartz, C. J. Lerche, T. Svanekjær, K. N. Kragh, A. S. Laulund, K. Thomsen, K. Å. Henneberg, T. Sams, N. Høiby, C. Moser, *J. Cystic Fibrosis* **2020**, *19*, 996.
[61] D. P. Pacheco, C. S. Butnarasu, F. Briatico Vangosa, L. Pastorino, L. Visai, S. Visentin, P. Petrini, *J. Mater. Chem. B* **2019**, *7*, 4940.
[62] C. Butnarasu, G. Caron, D. P. Pacheco, P. Petrini, S. Visentin, *Mol. Pharmaceutics* **2022**, *19*, 520.
[63] T. Bjarnsholt, P. Ø. Jensen, M. J. Fiandaca, J. Pedersen, C. R. Hansen, C. B. Andersen, T. Pressler, M. Givskov, N. Høiby, *Pediatr. Pulmonol.* **2009**, *44*, 547.
[64] B. J. Staudinger, J. F. Muller, S. Halldórsson, B. Boles, A. Angermeyer, D. Nguyen, H. Rosen, Ó. Baldursson, M. Gottfreðsson, G. H. Guðmundsson, P. K. Singh, *Am. J. Respir. Crit. Care Med.* **2014**, *189*, 812.
[65] D. Worlitzsch, R. Tarran, M. Ulrich, U. Schwab, A. Cekici, K. C. Meyer, P. Birrer, G. Bellon, J. Berger, T. Weiss, K. Botzenhart, J. R. Yankaskas, S. Randell, R. C. Boucher, G. Döring, *J. Clin. Invest.* **2002**, *109*, 317.
[66] P. Jorth, M. A. Spero, D. K. Newman, *mBio* **2019**, *10*, e02622.
[67] A. K. Wessel, T. A. Arshad, M. Fitzpatrick, J. L. Connell, R. T. Bonnecaze, J. B. Shear, M. Whiteley, *mBio* **2014**, *5*, e00992.
[68] M. Schobert, D. Jahn, *Int. J. Med. Microbiol.* **2010**, *300*, 549.
[69] J. R. W. Govan, J. W. Nelson, *Br. Med. Bull.* **1992**, *48*, 912.
[70] K. N. Kragh, J. B. Hutchison, G. Melaugh, C. Rodesney, A. E. L. Roberts, Y. Irie, P. Jensen, S. P. Diggle, R. J. Allen, V. Gordon, T. Bjarnsholt, *mBio* **2016**, *7*, e00237.
[71] Y. M. Cai, *Front. Microbiol.* **2020**, *11*, 557035.
[72] L. Yang, Y. Liu, T. Markussen, N. Høiby, T. Tolker-Nielsen, S. Molin, *FEMS Immunol. Med. Microbiol.* **2011**, *62*, 339.
[73] P. W. Woods, Z. M. Haynes, E. G. Mina, C. N. H. Marques, *Front. Microbiol.* **2019**, *9*, 3291.
[74] A. T. Nguyen, A. G. Oglesby-Sherrouse, *Appl. Microbiol. Biotechnol.* **2016**, *100*, 6141.
[75] A. R. Smyth, S. C. Bell, S. Bojcin, M. Bryon, A. Duff, P. Flume, N. Kashirskaya, A. Munck, F. Ratjen, S. J. Schwarzenberg, I. Sermet-Gaudelus, K. W. Southern, G. Taccetti, G. Ullrich, S. Wolfe, *J. Cystic Fibrosis* **2014**, *13*, S23.
[76] J. B. Lyczak, C. L. Cannon, G. B. Pier, *Clin. Microbiol. Rev.* **2002**, *15*, 194.
[77] H. S. Joo, M. Otto, *Chem. Biol.* **2012**, *19*, 1503.
[78] B. P. Conlon, S. E. Rowe, A. B. Gandt, A. S. Nuxoll, N. P. Donegan, E. A. Zalis, G. Clair, J. N. Adkins, A. L. Cheung, K. Lewis, *Nat. Microbiol.* **2016**, *1*, 16051.
[79] J. X. Huang, M. A. T. Blaskovich, R. Pelingon, S. Ramu, A. Kavanagh, A. G. Elliott, M. S. Butler, A. B. Montgomery, M. A. Cooper, *Antimicrob. Agents Chemother.* **2015**, *59*, 5925.
[80] C. T. Huang, K. D. Xu, G. A. McFeters, P. S. Stewart, *Appl. Environ. Microbiol.* **1998**, *64*, 4035.
[81] E. Kamble, K. Pardesi, *Microb. Drug Resist.* **2021**, *27*, 3.
[82] A. P. Magalhães, S. P. Lopes, M. O. Pereira, *Front. Microbiol.* **2017**, *7*, 2146.
[83] P. Briaud, L. Camus, S. Bastien, A. Doléans-Jordheim, F. Vandenesch, K. Moreau, *Sci. Rep.* **2019**, *9*, 16564.
[84] X. Wang, S. Koehne-Voss, S. S. Anumolu, J. Yu, *J. Pharm. Sci.* **2017**, *106*, 3402.
[85] S. Magréault, J. Mankikian, S. Marchand, P. Diot, W. Couet, T. Flament, N. Grégoire, *J Cystic Fibrosis* **2020**, *19*, 421.
[86] B. Lamy, F. Tewes, D. R. Serrano, I. Lamarche, P. Gobin, W. Couet, A. M. Healy, S. Marchand, *J. Controlled Release* **2018**, *271*, 118.
[87] E. Secchi, T. Roversi, S. Buzzaccaro, L. Piazza, R. Piazza, *Soft Matter* **2013**, *9*, 3931.
[88] R. Piazza, In *Colloidal Foundations of Nanoscience*, Elsevier, Amsterdam, **2014**, pp. 233–266.
[89] A. Bari, N. Bloise, S. Fiorilli, G. Novajra, M. Vallet-Regí, G. Bruni, A. Torres-Pardo, J. M. González-Calbet, L. Visai, C. Vitale-Brovarone, *Acta Biomater.* **2017**, *55*, 493.
[90] S. Schenk, *FEMS Microbiol. Lett.* **1992**, *94*, 133.
[91] F. Cadoret, C. Soscia, R. Voulhoux, In *Pseudomonas Methods and Protocols*, (Eds.: A. Filloux, J. Ramos), Springer Protocols, Humana Press, New York, **2014**, pp. 11–15.
[92] M. Sharifian Gh, *Mol. Pharmaceutics* **2021**, *18*, 2122.

© 2023 The Authors. Advanced Functional Materials published by Wiley-VCH GmbH

16163028, 2023, 50, Downloaded from https://advanced.onlinelibrary.wiley.com/doi/10.1002/adfm.202306116 by CochraneItalia, Wiley Online Library on [26/10/2025]. See the Terms and Conditions (https://onlinelibrary.wiley.com/terms-and-conditions) on Wiley Online Library for rules of use; OA articles are governed by the applicable Creative Commons License